Master's Thesis

A Study on the Effect of Current Density on the Internal Short by Cu Contaminants in the Lithium-ion Battery Using In-Situ Optical Microscopy

Changhun Sung

Department of Energy Engineering

(Battery Science and Technology)

Graduate School of UNIST

2019

A Study on the Effect of Current Density on the Internal Short by Cu Contaminants in the Lithium-ion Battery Using In-Situ Optical Microscopy

Changhun Sung

Department of Energy Engineering
(Battery Science and Technology)

Graduate School of UNIST

A Study on the Effect of Current Density on the Internal Short by Cu Contaminants in the Lithium-ion Battery Using In-Situ Optical Microscopy

A thesis/dissertation
submitted to the Graduate School of UNIST
in partial fulfillment of the
requirements for the degree of
Master of Science

Changhun Sung

01/03/2019
Approved by

Advisor
Kyeong-Min Jeong

A Study on the Effect of Current Density on the Internal Short by Cu Contaminants in the Lithium-ion Battery Using In-Situ Optical Microscopy

Changhun Sung

This certifies that the thesis/dissertation of Changhun Sung is approved.

01/03/2019

Advisor: Kyeong-Min Jeong

Hyun-Kon Song

Hyun-Wook Lee

Contents

Abstract

Lithium-ion batteries are composed of various metal materials such as aluminum substrate, copper substrate, Al tab and Ni tab as well as cathode material, anode material, electrolyte and separator. Lithium-ion batteries have been exposed to various metal contaminations such as brass, copper, zinc, iron during manufacturing process. In addition, when a nickel-based cathode active material and copper tab are applied to satisfy a high energy density, the possibility of the influence of metal contaminations is increased. The metal contaminations cause internal-short in the lithium-ion cell that reduces the voltage of the charged cell. In the case of a battery for electric vehicles and ESS, several cells are connected in series or parallel for high power and capacity. Under the influence of the voltage drop of a few cells by the internal short by metal contaminations, other cells are exposed at risk of overcharging.

In this research, we studied the internal short when there was Cu contamination on the surface of cathode. By using in-situ optical microscopy, behavior of dissolution and deposition of Cu was observed at certain current. The self-discharge phenomenon in the presence of a Cu contamination on the positive electrode was confirmed. Also, by investigating the difference in the behavior of Cu contamination according to the charge current density, we sought a way to reduce the voltage drop problem by the internal short when there is Cu contamination.

List of Figures

I. Introduction

1.1. Lithium-ion batteries

The lithium-ion battery has been used as one of the main products supporting the ubiquitous society. In the early days of development, it was applied to small electronic devices. A need for high gravimetric energy density and power density for electric vehicles and energy storage systems has been increased. Figure 1 shows lithium-ion batteries have higher specific energy and power comparison with other batteries like lead-acid, nickel-cadmium batteries.

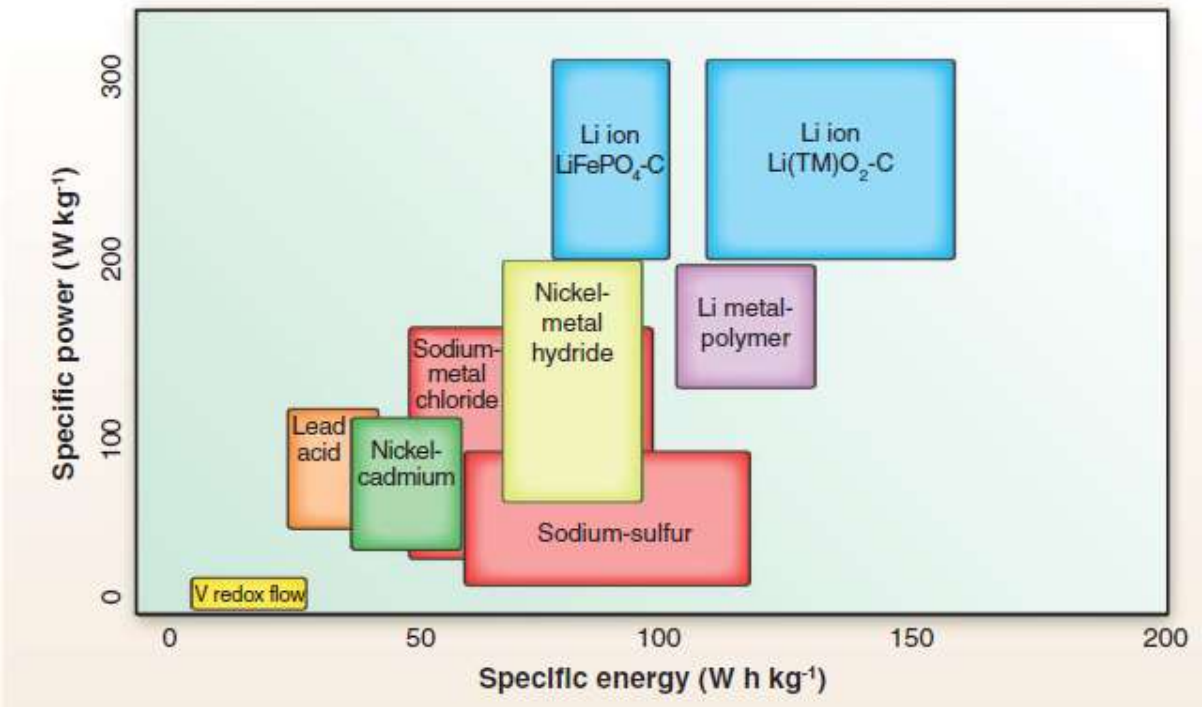

Figure 1 Gravimetric power densities and energy densities for different rechargeable batteries. [1]

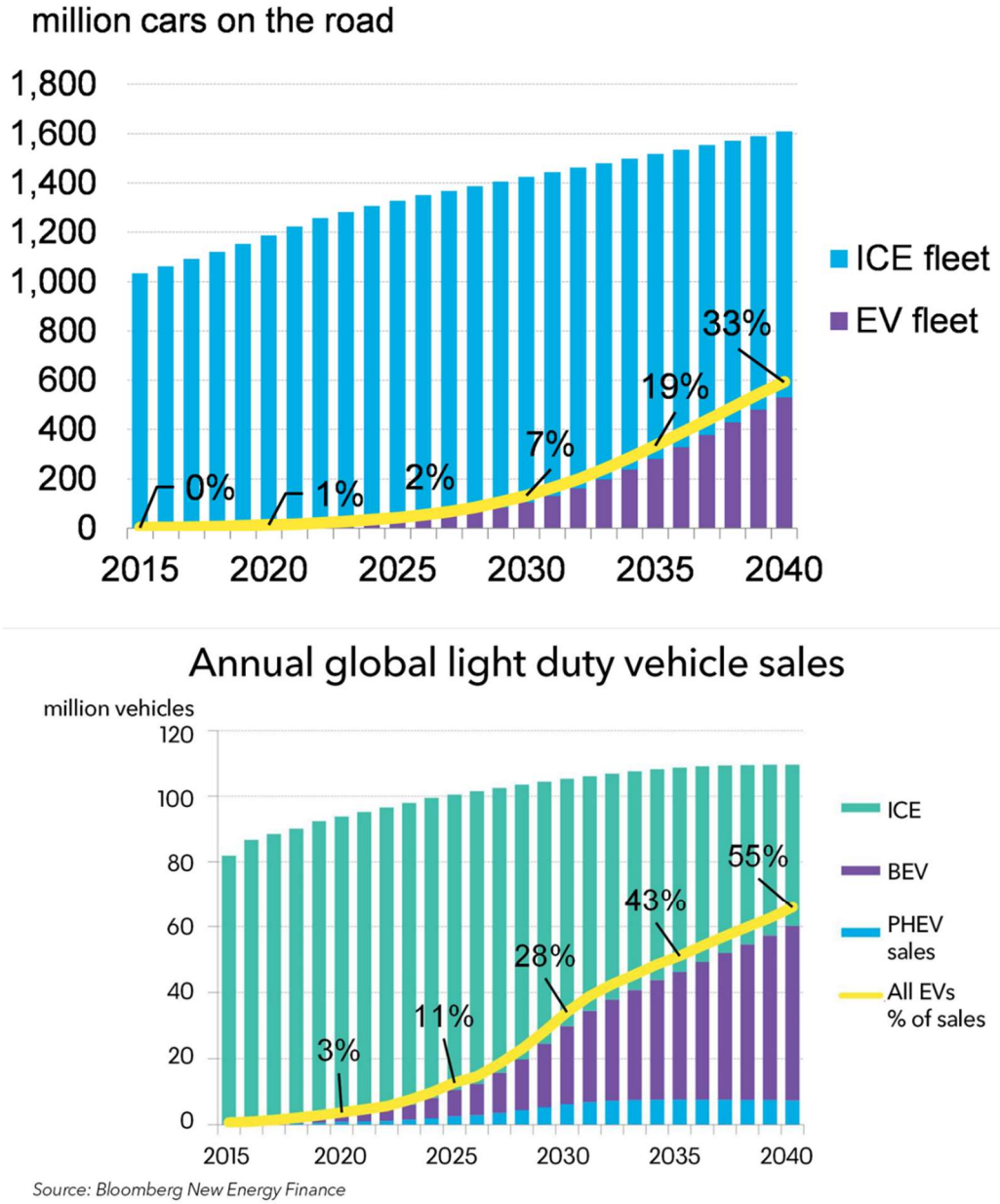

Figure 2 Annual global light duty vehicle sales and global light duty vehicle fleet, Bloomberg report.

https://about.bnef.com/blog/electric-vehicles-accelerate-54-new-car-sales-2040/

Bloomberg predicts that the share of electric vehicles on the road will increase to 33 % and small-sized electric vehicle sales, which are currently 1%, will increase to 54% in 2040, exceeding that of internal combustion engines, as battery prices decline.

1.2. Internal short in lithium-ion batteries

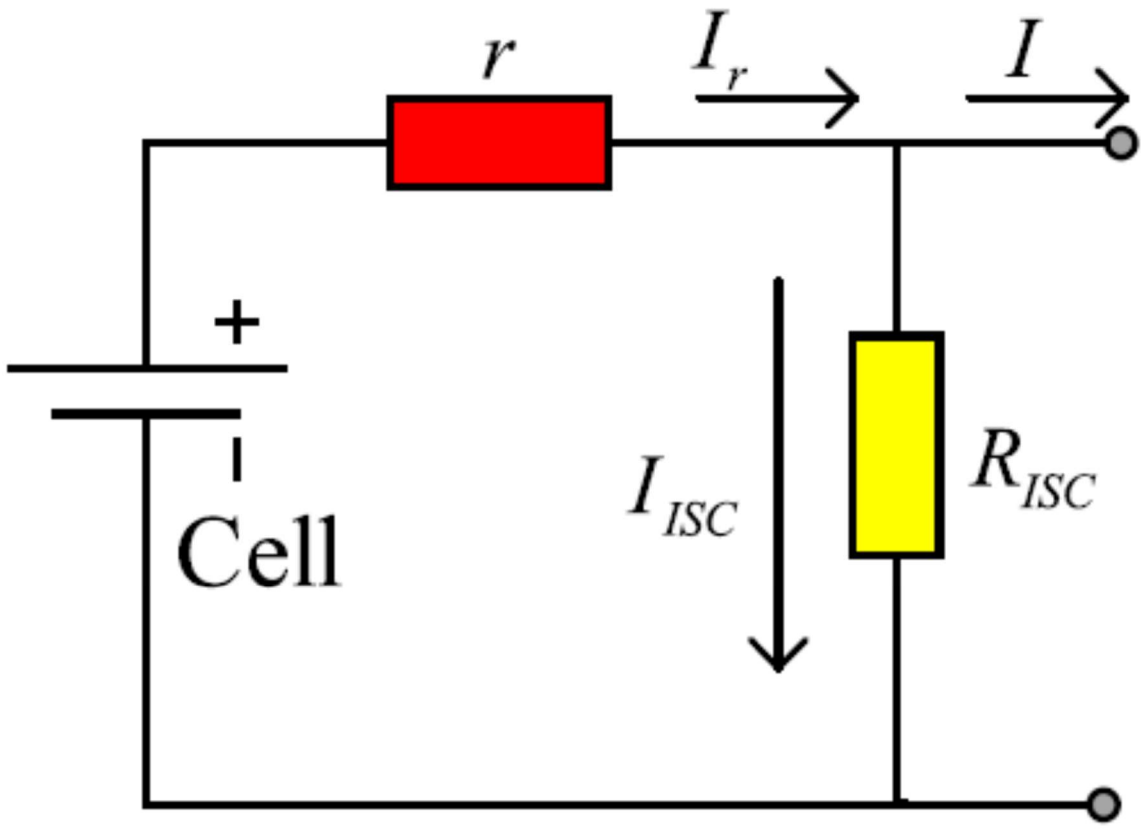

Figure 3 Electrical representation of internal short circuit. [5]

For the normal cell that has not an internal short circuit, resistance of the internal short circuit is infinite, then there is no leakage current. However, if there is the internal short, resistance of the internal short circuit is very lower comparison with internal resistance that causes self-discharging problem and heat generation[6-9]. There are several factors that cause the internal shorts such as physical nail penetration, lithium dendrite and over-discharge. The internal short in lithium-ion batteries cause lower SOC cell in a series of lithium-ion batteries and heat generation by high current flow on the internal short. Figure 4 shows the effect of low-SOC cell by the internal short on a system connected in series with a lithium-ion battery. During charging and discharging lithium-ion modules, low-SOC cell affects other normal cells. For cell voltage control system, during discharging process, other cells were discharged enough by lower cell voltage limit of low-SOC cell. In case of average voltage control system, during charging process, other cells were over-charged under the influence of low potential of low-SOC cell.

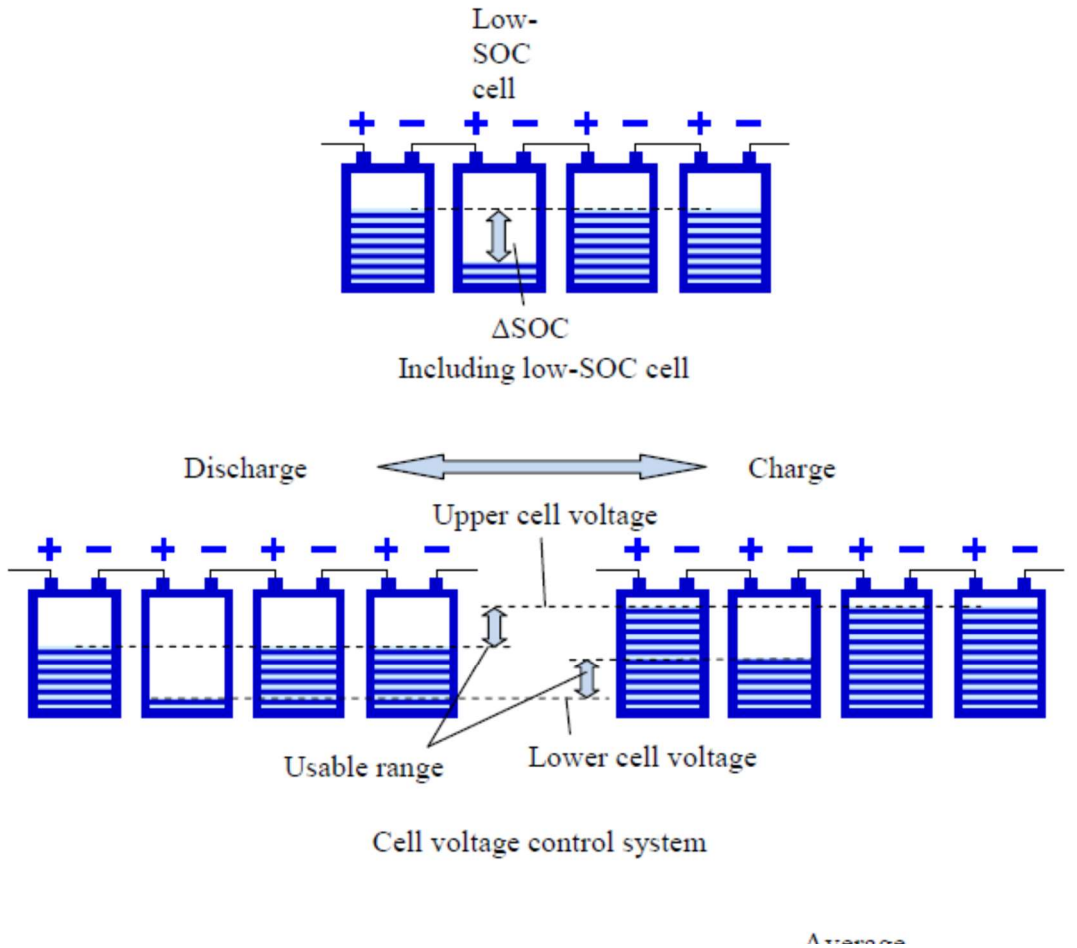

Figure 4 Electrical representation of internal short circuit. [5]

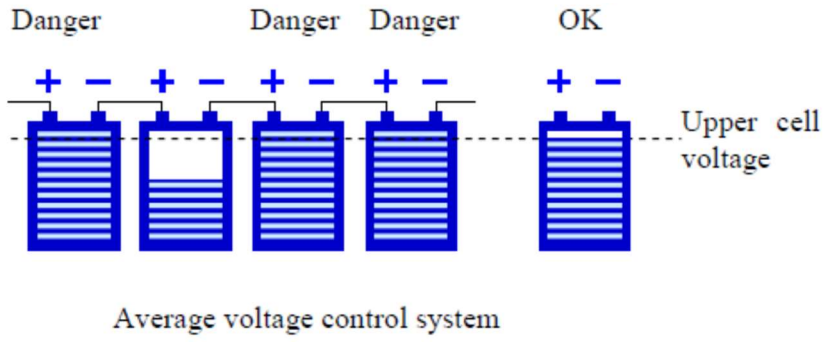

Figure 4 Schematic illustration of danger of low-SOC cell by internal shorts in series with a lithium-ion battery. [2]

1.2.1. Over-discharge

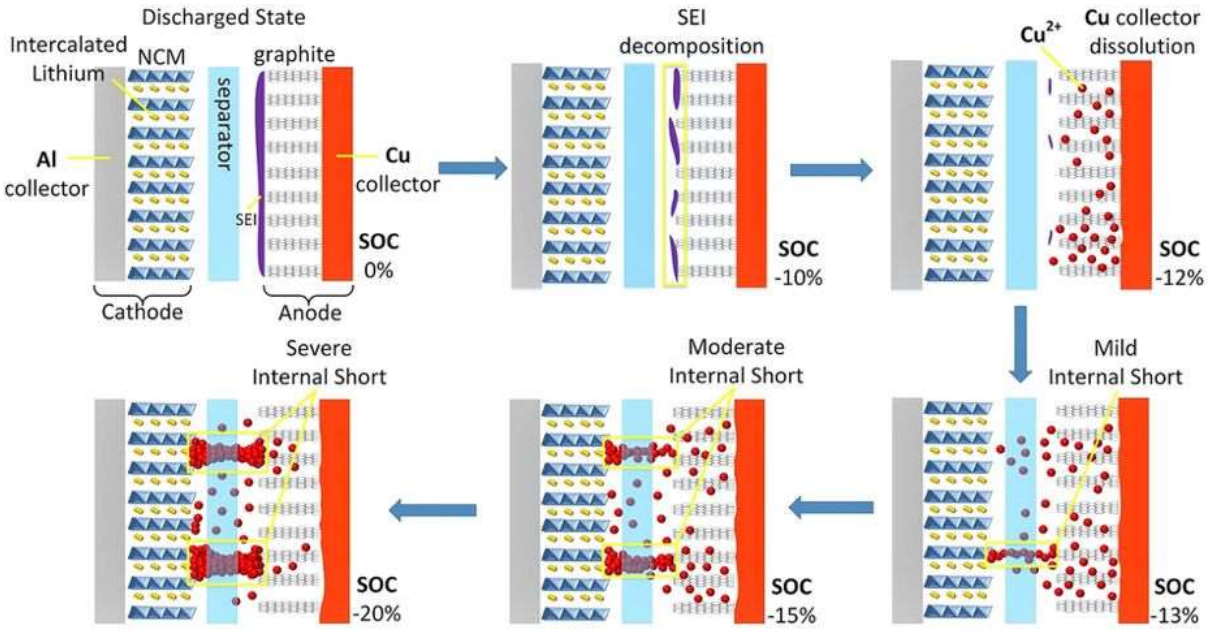

Figure 5 Mechanism of internal short circuit's formation by Cu current collector dissolving during over-discharging. [4]

Lithium-ion cell has been connected in series to satisfy high voltage for electric vehicles. Over-discharge is one of commons abuse cases of lithium-ion batteries. Cu current collector is stable during normal charging and discharging process. However, Cu current collector is oxidized to Cu^{2+} during over-discharging, dissolved Cu^{2+} is deposited on surface of cathode, and the internal short occurs as shown in figure 5. Potential of anode is in range between 0 V and 0.8 V during normal charging and discharging process. Since the redox potential of Cu metal is more than 3 V compared to lithium redox potential, oxidation does not occur in the normal charge and discharge process. However, abnormally during over-discharging, potential of anode increases up to 5 V as shown in figure 7. The potential of anode is higher than redox potential of Cu, so that the Cu current collector is dissolved. Difference of electrode between fresh cell and over-discharged cell can be shown in figure 8. In fresh cell, there is no crack and damage on surface of electrode. However, in case of over-discharged cell, surface of anode cracked, and Cu current collector was thinner than that of fresh cell. That made reduce the mechanical stability of the anode and increase the charge transfer resistance of the cell. Although Al current collector did not crack, surface of cathode electrode was covered with Cu. This Cu deposition comes from Cu current collector of anode electrode. As the higher degree of discharge during over-discharge, The degree of the internal short circuit increases. Figure 9 indicated voltage drop difference as degree of discharge.

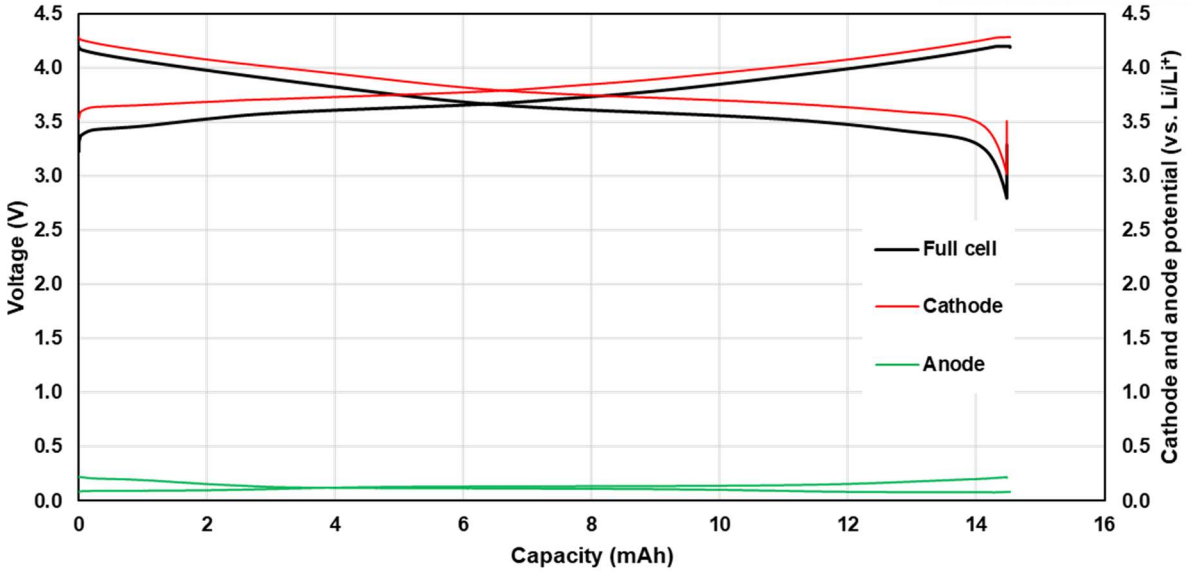

Figure 6 Voltage of full cell, potential of cathode and anode during normal charging and discharging process.

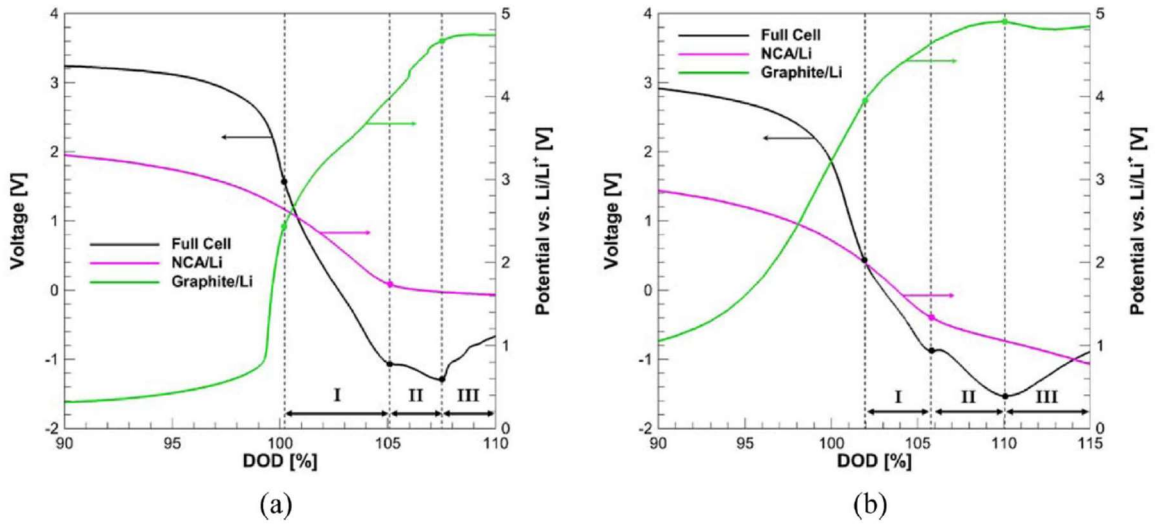

Figure 7 Voltage of full cell, potential of cathode and anode during over-discharging. [3]

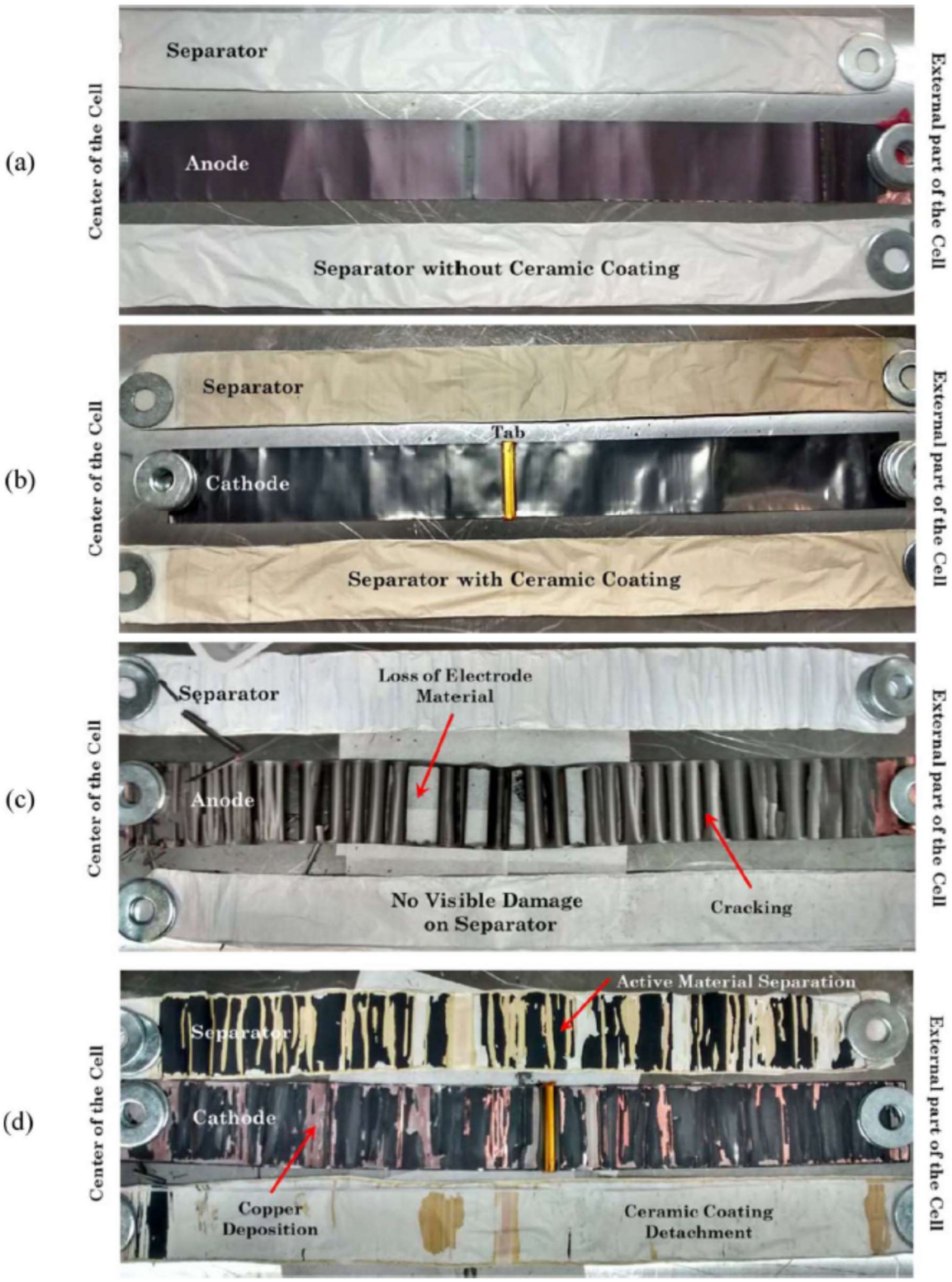

Figure 8 Cathode, anode and separator post-mortem photo of fresh cell and over-discharged cell.[3]

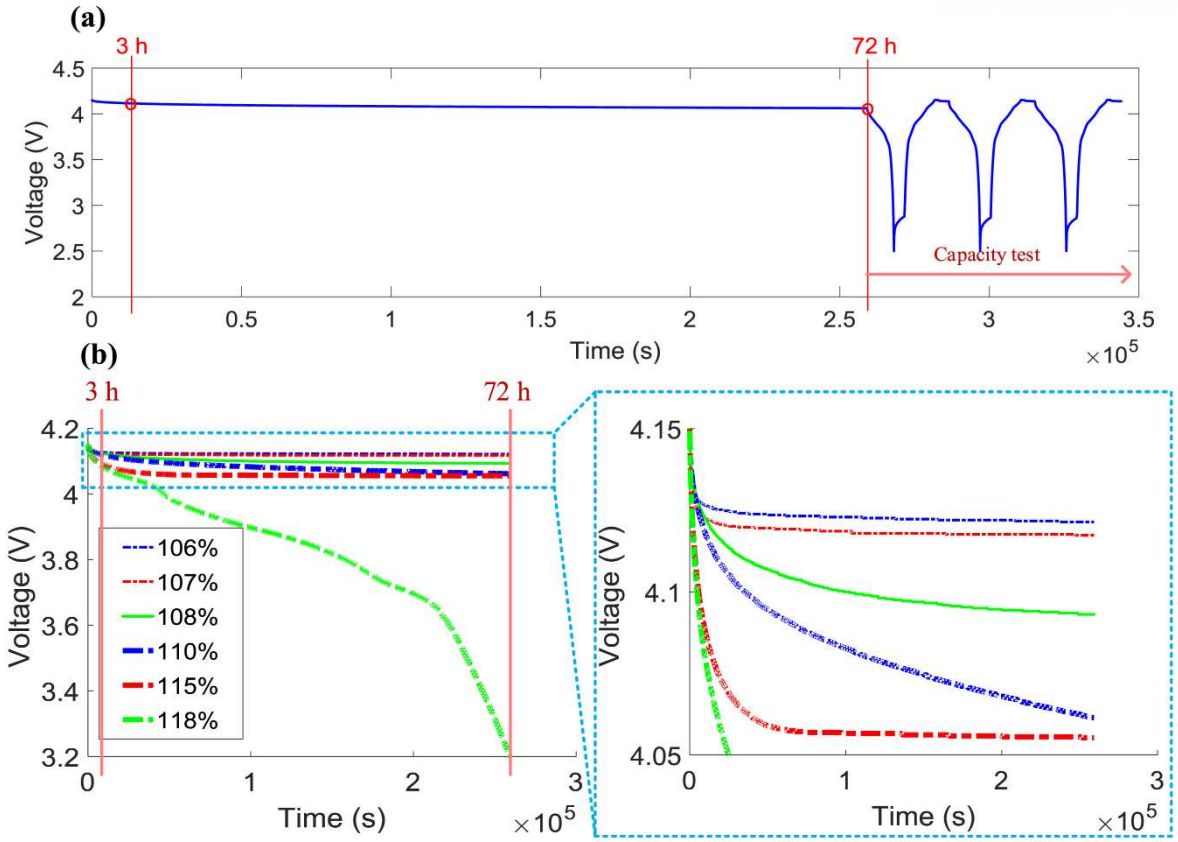

Figure 9 Voltage variations of over-discharged cell after 4.2 V charging. [5]

1.2.2. Cu contaminations

Lithium-ion batteries manufacture process is exposed to metal contamination such as iron, brass, copper, zinc, aluminum. These metal contaminations were dissolved during charging process, that makes the internal short in cell. The internal short in cell causes low-SOC cell. Degree of dissolution of metal contaminations is difference according to species of metal because of difference of redox potential of metal, as shown in figure 10. This makes difference of degree of effect of the internal short by metal contamination according to species of metal contamination, Figure 11 shows degree of effect of the internal short follows the redox potential of each metal contamination.

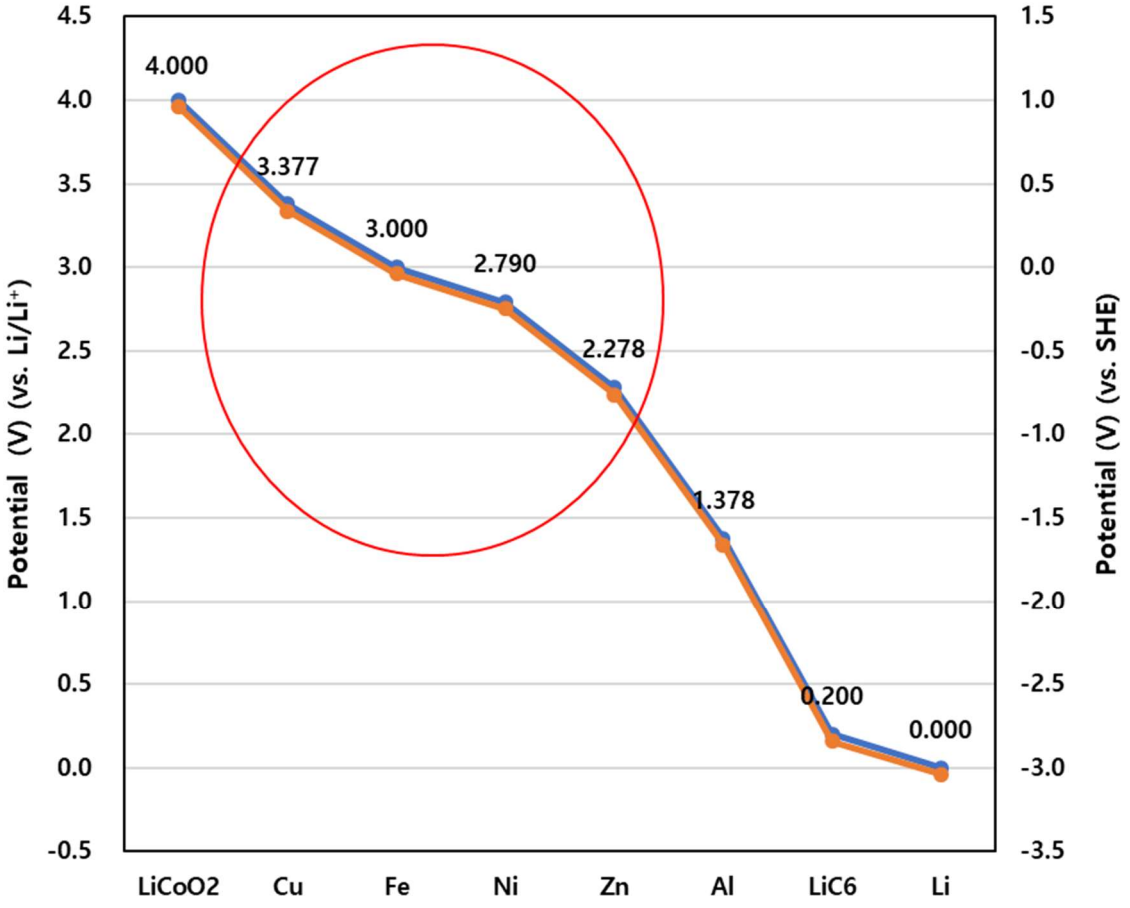

Figure 10 Redox potential according to species of metal.

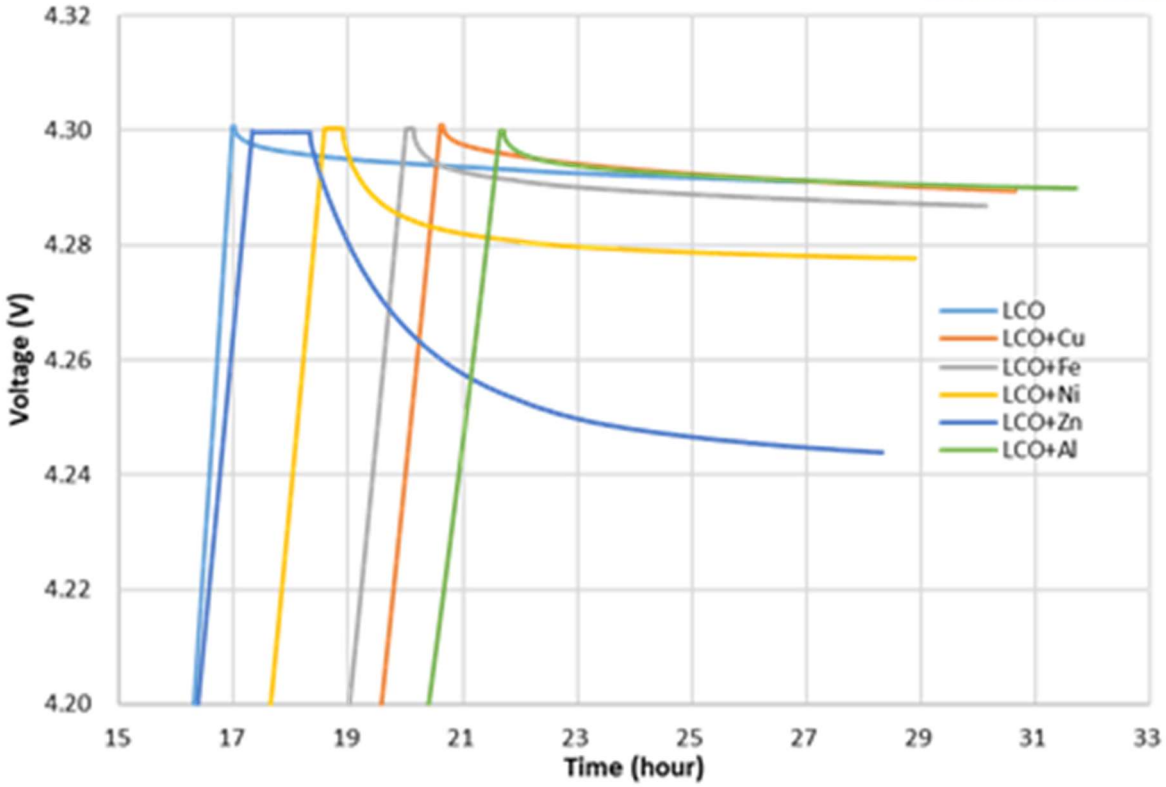

Figure 11 Difference of degree of voltage drop according to metal species in LCO cathode.

Junju Kuwabara studied about formation of the internal short by Cu contamination.[2] Cu contamination was dissolved after 2 minutes after stating charging to full cell. At initial of charging, cell voltage under 3 V, however, Cu contamination was dissolved that redox potential of Cu is 3.3 V comparing with Li redox potential. Cell voltage is difference between potential of cathode and anode. Because cathode potential was over 3.3 V at initial of charging, Cu was dissolved as soon as starting charging. Figure 12 shows effect of the internal short by Cu contamination during charging process and figure 13 shows image of growth of Cu on anode while charging process. The internal short makes local low-SOC area by self-discharge. The local low-SOC area was charged during constant voltage charge process as shown in figure 14. After charged local low-SOC area, Cu was re-dissolved because potential of this area is increased over redox potential of Cu.

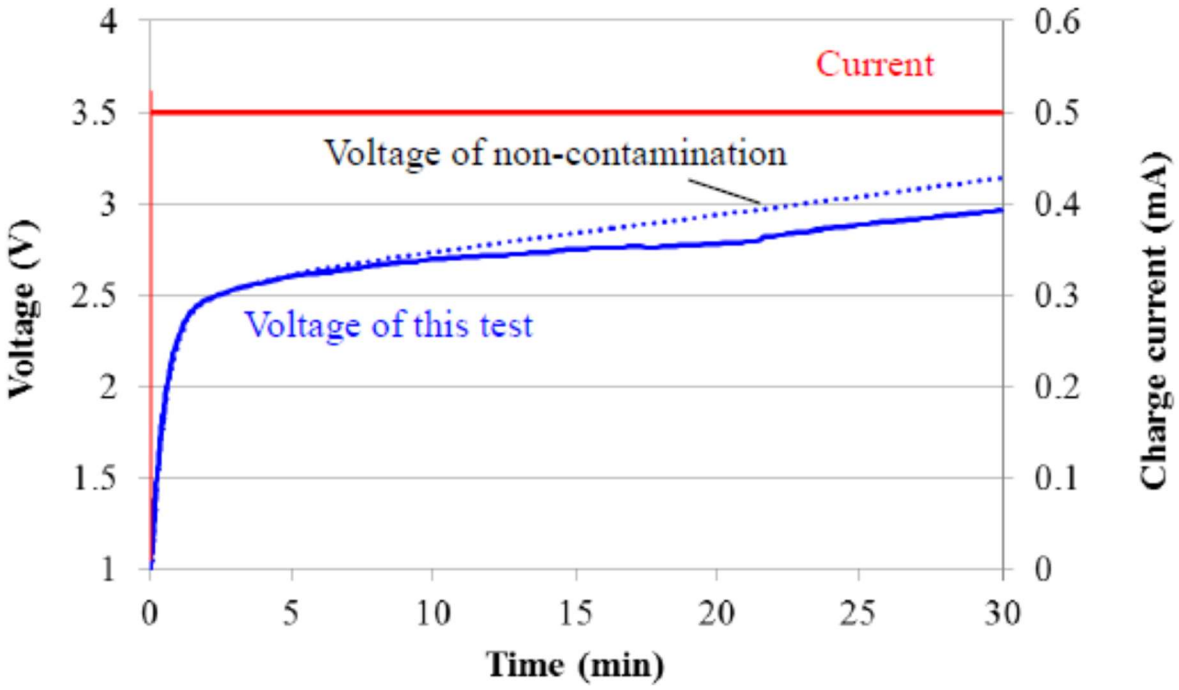

Figure 12 Voltage profile of full cell depending on whether Cu contamination is present or not in cathode during constant current charge. [2]

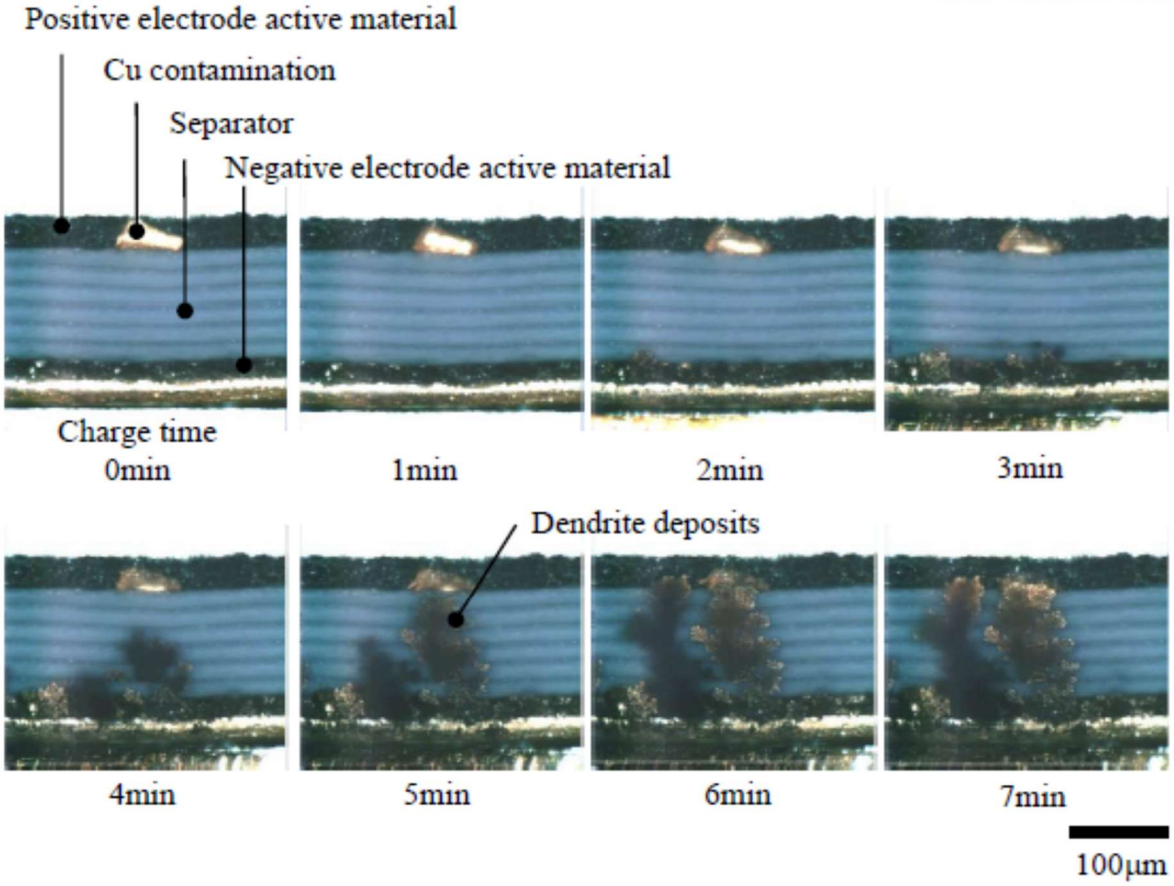

Figure 13 in-situ image of full cell when Cu contamination is present in cathode during constant current charge. [2]

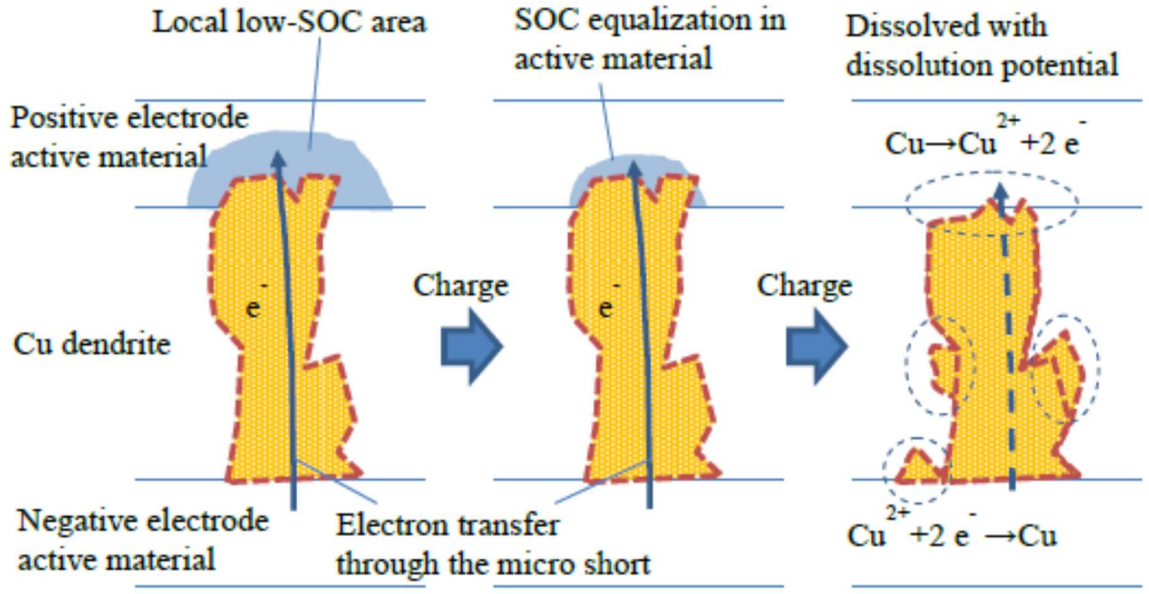

Figure 14 image diagram of Cu re-dissolving during constant voltage charging. [2]

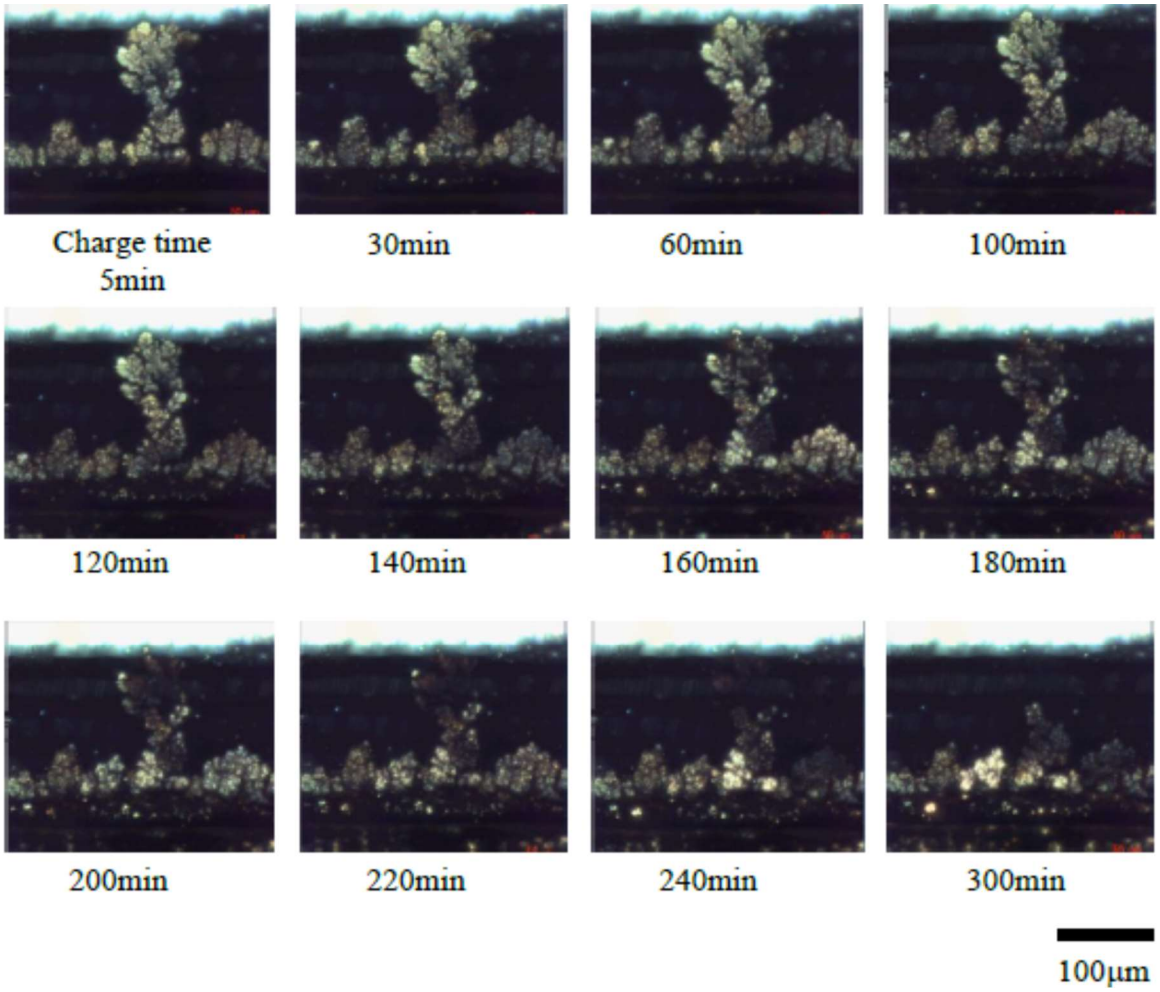

Figure 15 in-situ image of full cell when Cu contamination is present in cathode during constant voltage charge. [2]

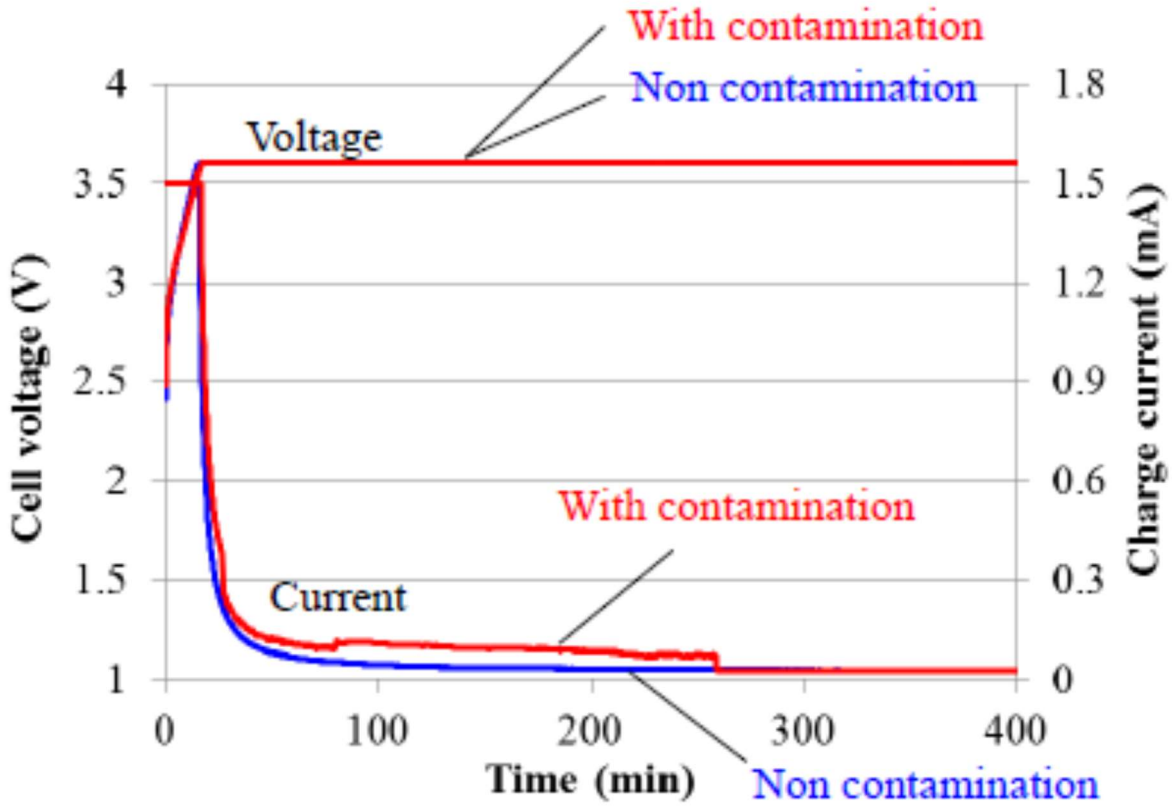

Figure 16 Voltage profile of full cell depending on whether Cu contamination is present or not in cathode during constant voltage charge. [2]

II. Experimental Method

2.1. Electrode manufacturing

NCM622 (L&F Co., Ltd.) and S360 (BTR Ltd.) graphite were used as cathode and anode material. Positive electrodes were prepared with 2 % Super P and 2 % PVDF binder. Three components were mixed in homogenizer with 10000 rpm for 45 min. The mixed slurry was coated on 31 um thick aluminum foil. The mixed slurry was applied on aluminum at a loading level of 17 mg/cm^2, dried in a convection oven at 110 ^{o}C for 1 hour and roll pressed to 3.3 g/cc. It was dried in 110 ^{o}C vacuum oven for 10 hours. In the case of a positive electrode containing Cu contamination, several hundreds of micro-level Cu sheets were put on the positive electrode before pressing process, then pressed with composite. Negative electrode was mixed with 1.2 % CMC, 1.4 % SBR binder in homogenizer with 12000 rpm for 1 hour. The mixed slurry was coated to 9.5 mg/cm^2 on 22 um thick copper foil and pressed to 1.6 g/cc after drying the convection oven at 110 ^{o}C for 1hour. As with the positive electrode, negative electrode was dried in a 110 ^{o}C vacuum oven for 10 hours.

2.2. LSV, potential step experiment

LSV experiment and potential step experiment were used 1 x 1 cm^2 Cu plate as working electrode, Li metal as counter electrode and reference electrode. LSV and potential step experiment were measured by VSP-300, Biologic EC-Lab. In case of LSV, scan rate was 1 mV/sec from 3.0 V to 3.8 V. Potential step experiment was measured in 0.1 V intervals from 3.4 V until current density exceeds 1000 mA/cm^2.

2.3. In-situ optical microscopy

Optical microscopy (BX53M, OLYMPUS) and Optical test cell (ECC-opto-SBS, EL-CELL) were used to observe Cu dissolution and deposition in electrolyte during applying constant current. Cu foil was used as working electrode, counter electrode and Li metal was used reference electrode in the optical test cell.

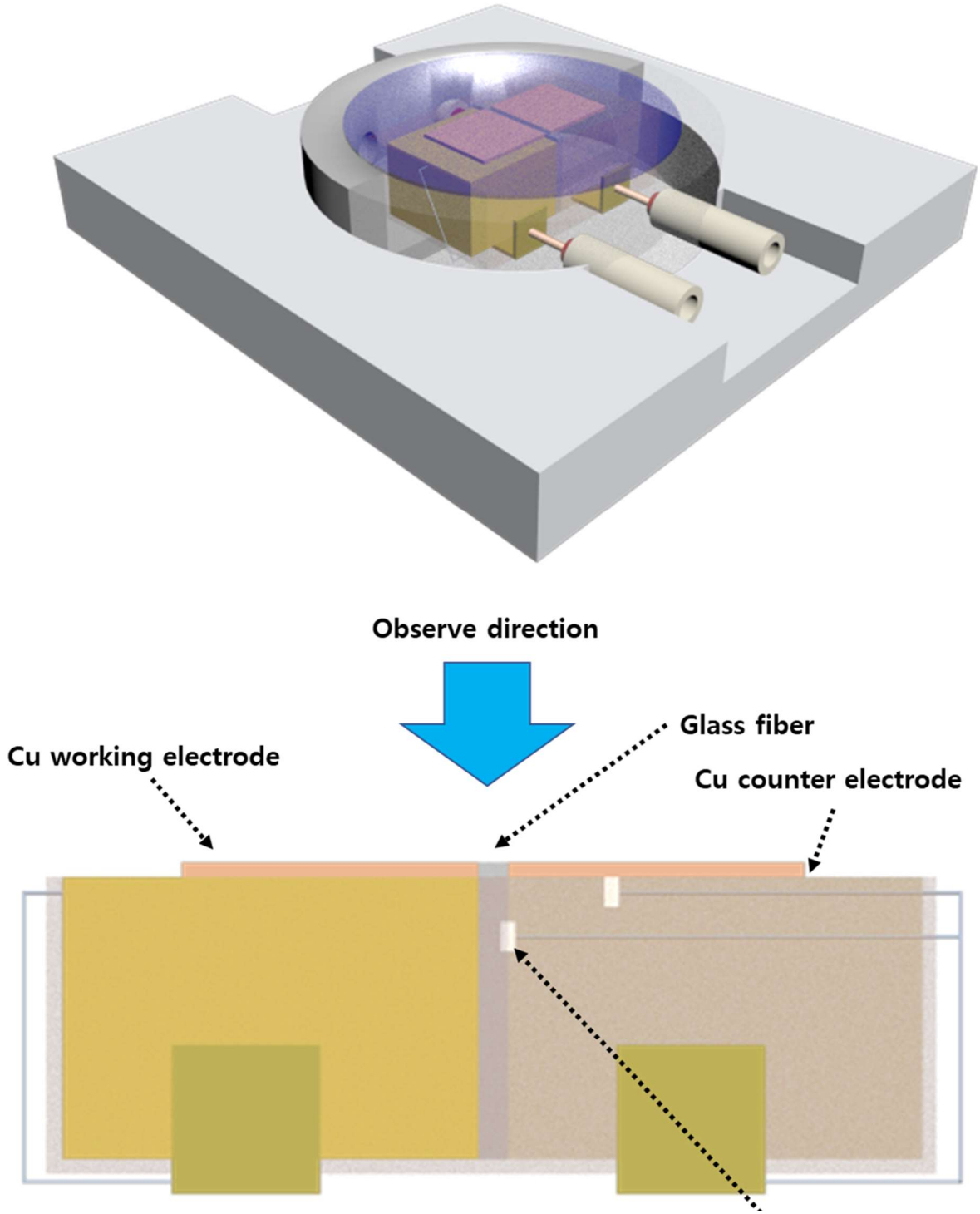

Figure 17 Image diagram of optical test cell.

2.4. Half-cell manufacturing and test

The cathode was tested in 2032-coin half-cell assembled in dry room. 4 separators were used in half-cell for observing internal short phenomenon. Charge and discharge cycles were done by PNE SOLUTION. To identify the difference in the behavior of Cu contamination on cathode with the current density, the cathode half-cell was charged to 4.3V in difference of constant current density and 1/50 C constant voltage charging after cell manufacturing and 10-hour rest. Half-cell was observed during 24-hours rest without current.

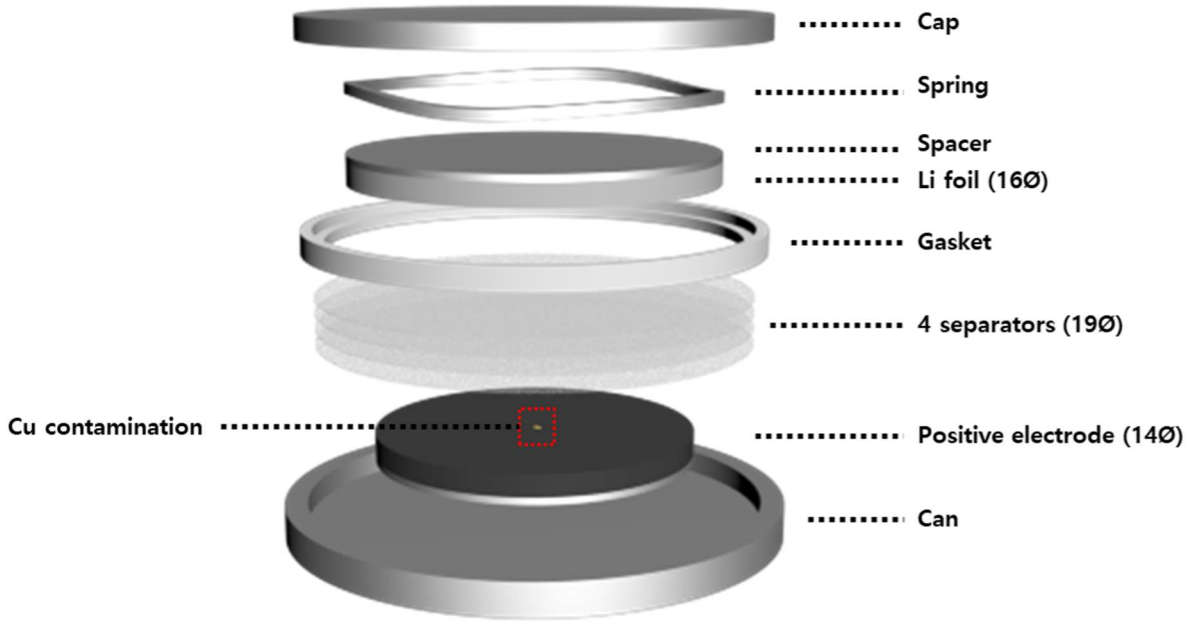

Figure 18 Image diagram of 2032 coin half-cell using 4 separators.

2.5. GITT

After Charging, GITT measurements were performed by applying 50 times of discharge current pulse at 1/20 C-rate for 10 min followed by rest time for 30 minutes. Because initial change of potential during discharge was high, low current density was applied. After 50 times of pulse at 1/20 C-rate, 50 times of discharge current pulse at 1/10 C-rate for 10 min followed by rest time for 2 hours.

III. Result and Discussions

3.1 Copper redox potential and shape of deposition

3.1.1. Redox potential of Cu metal in electrolyte containing Li salt

Redox potential and reaction current at certain voltage of copper in aqueous solution were well known. But lithium-ion batteries used organic solution and there is no Cu ion. LSV data shows the redox potential of cupper (vs. Li/Li^+) in the organic electrolyte and reaction current density at the charge potential range of the cathode material. From 3.3 V (vs. Li/Li^+), oxidation of Cu is started, Cu^{2+} ion moved and deposited on Li counter electrode. After 3.7 V, current density of anodic reaction beyond the 1 mA/cm^2. The deposited Cu grew until reaching working electrode. After LSV test, open circuit voltage of cell did not maintain equal voltage before test (3.3 V), similarly to 0 V by the internal short from Cu deposition on counter electrode. In charge process of lithium-ion batteries, Cathode potential increases up to 4.3 V, that means cathode potential will maintain to dissolve Cu contaminations.

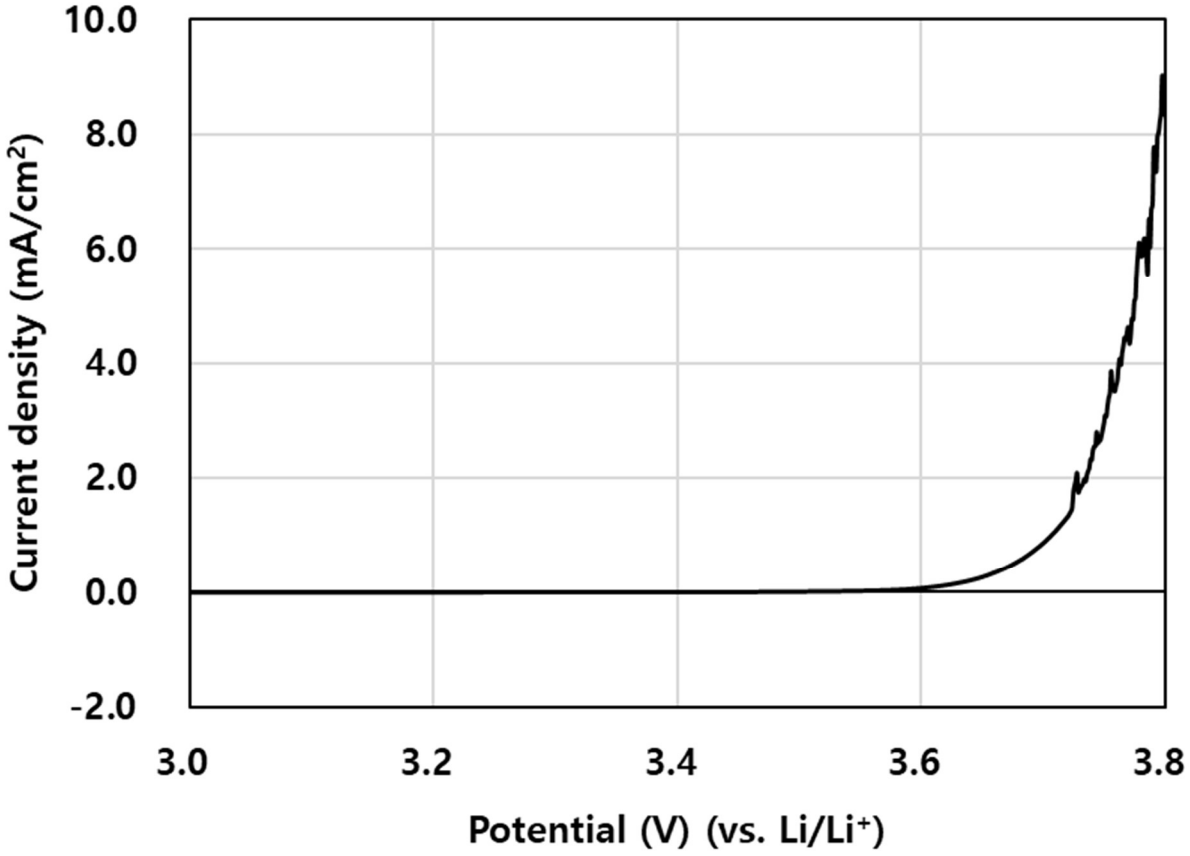

Figure 19 Result of linear sweep voltammetry using Cu/Li pouch cell.

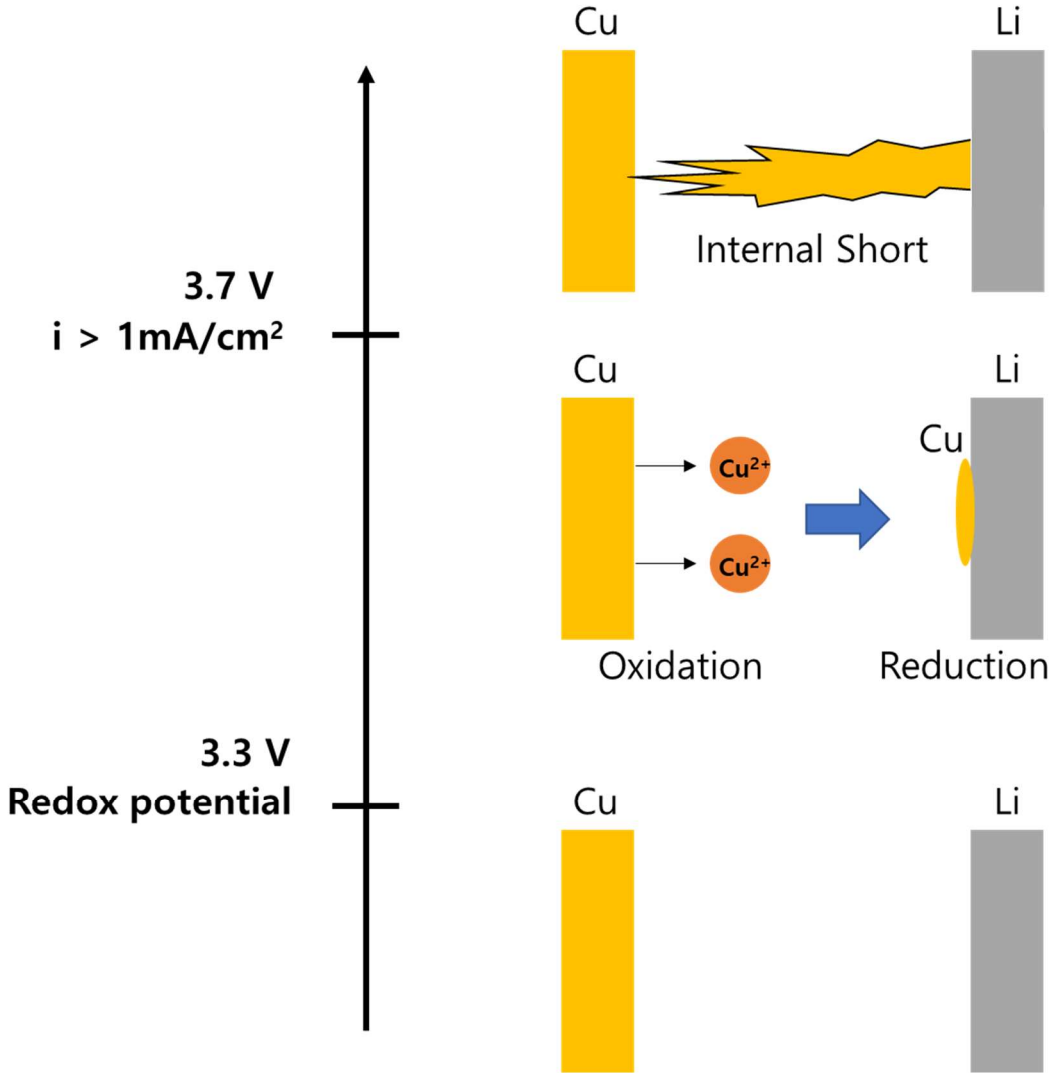

Figure 20 Schematic image of Cu dissolution, deposition and internal short.

3.1.2. Observation of copper deposition

Figure 21 shows Cu dissolution and deposition behavior according to the current of 10uA, 50uA, 100uA. Figure 22 indicates change of voltage and current during constant current. After starting to apply current, Cu of working electrode was dissolved, and lithium was deposited on anode. Electrolyte contained lithium salt, not Cu. As Cu was oxidized, Li was reduced on counter electrode. After Cu was dissolved enough, Cu ion moved to counter electrode, deposited on surface of counter electrode. As the applied current increases, the deposition rate of copper increases, equilibrium potential of Cu increases. Because the time for moving Cu ion to counter electrode is same, initial Li deposition is more as current is high.

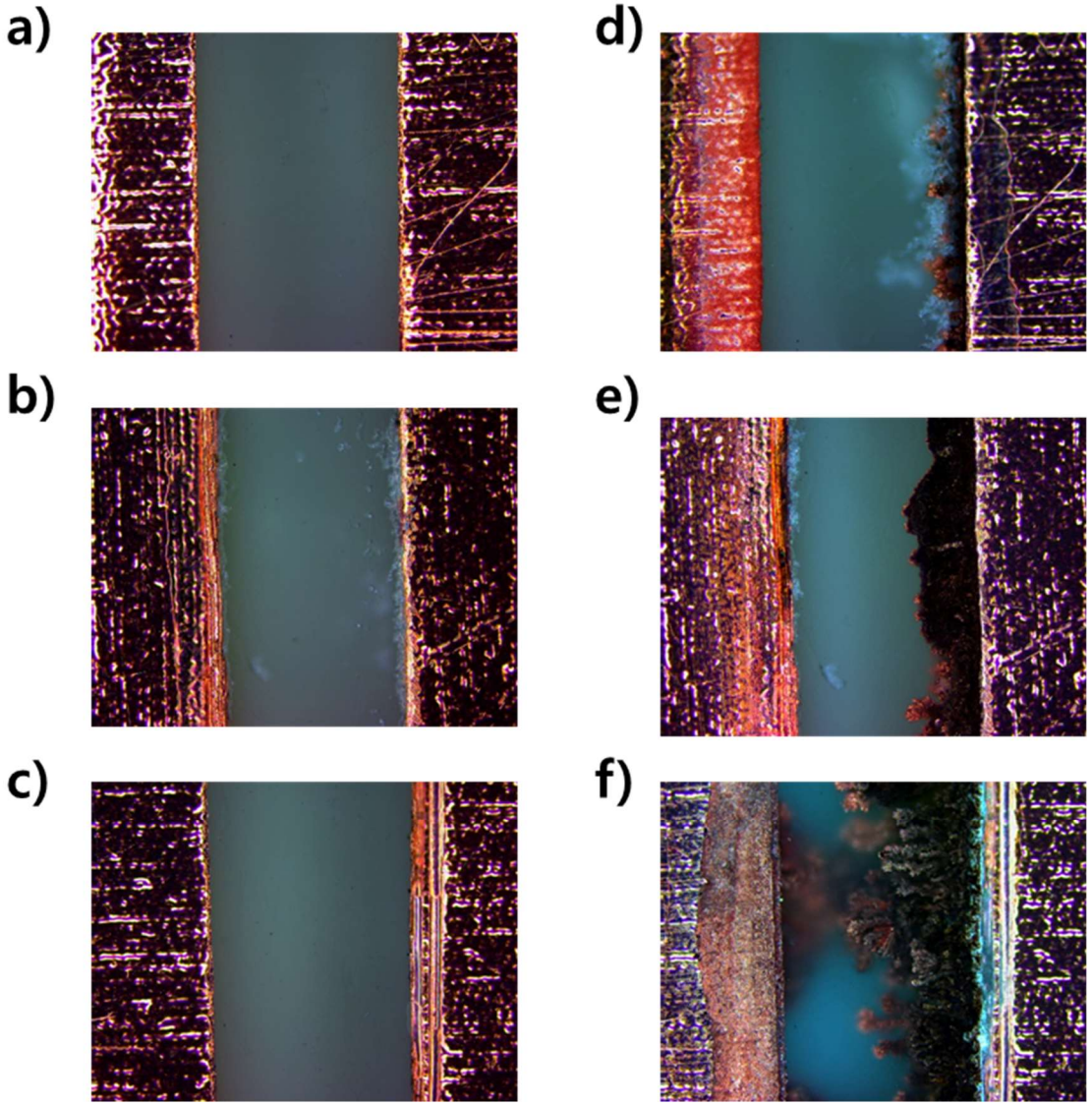

Figure 21 In-situ photo of Cu dissolution and deposition as different current. Cu/Cu in-situ symmetric cell before applied a) 10uA, b) 50uA and c) 100uA, after applied d)10uA, e) 50uA, and f) 100uA current.

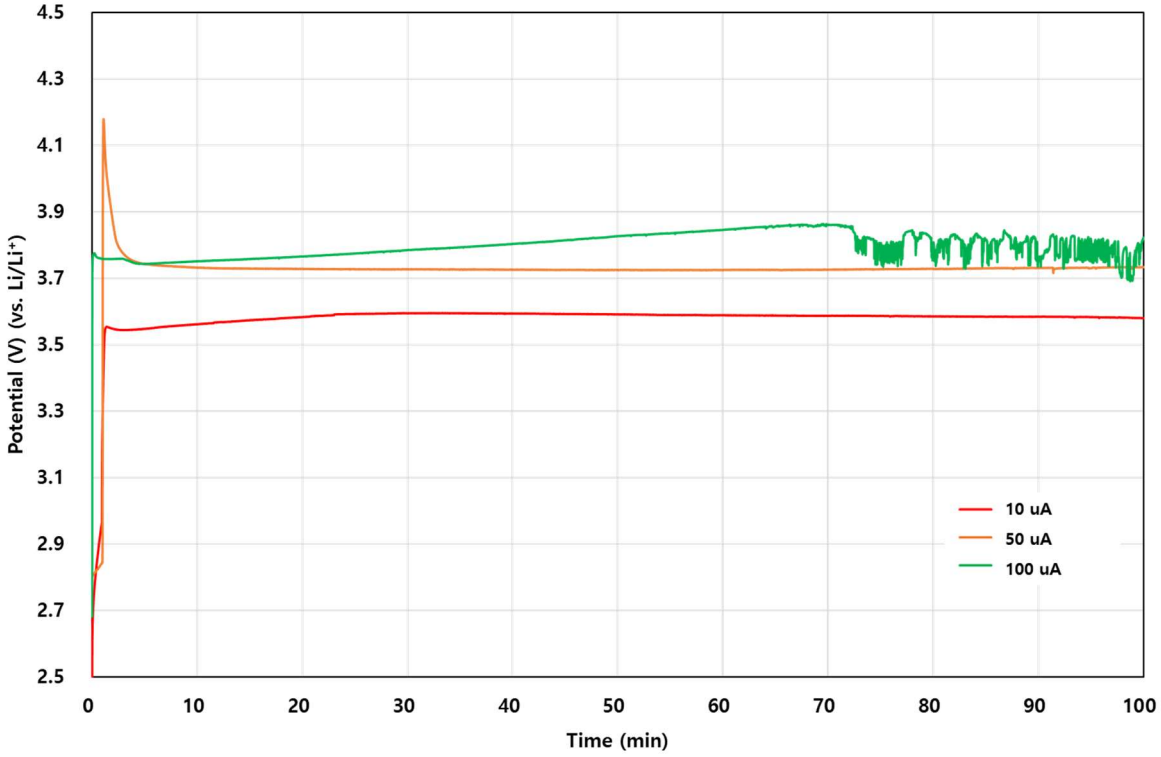

Figure 22 Variation of potential of Cu according to applied current.

3.2. Half-Cell

3.2.1. Difference of state of charge as current density

Figure 23 shows difference of voltage profile as current density. Because of overpotential by difference of current density, as higher current density was applied, as higher potential was maintained at similar state of charge during constant current charging. Gap of capacity as current density reduces during constant voltage charging. As higher current density was applied at constant current charging, it takes much longer time during constant voltage charging. The final capacity of cells as current density at first cycle is all similar after constant current and constant voltage charging. Figure 24 indicates current density until 1.5 mA/cm^2 did not have a large influence on capacity. For 24-hour rest after charging, potential of cathode was maintained from 4.26 V to 4.28 V, that means state of charge is all similar.

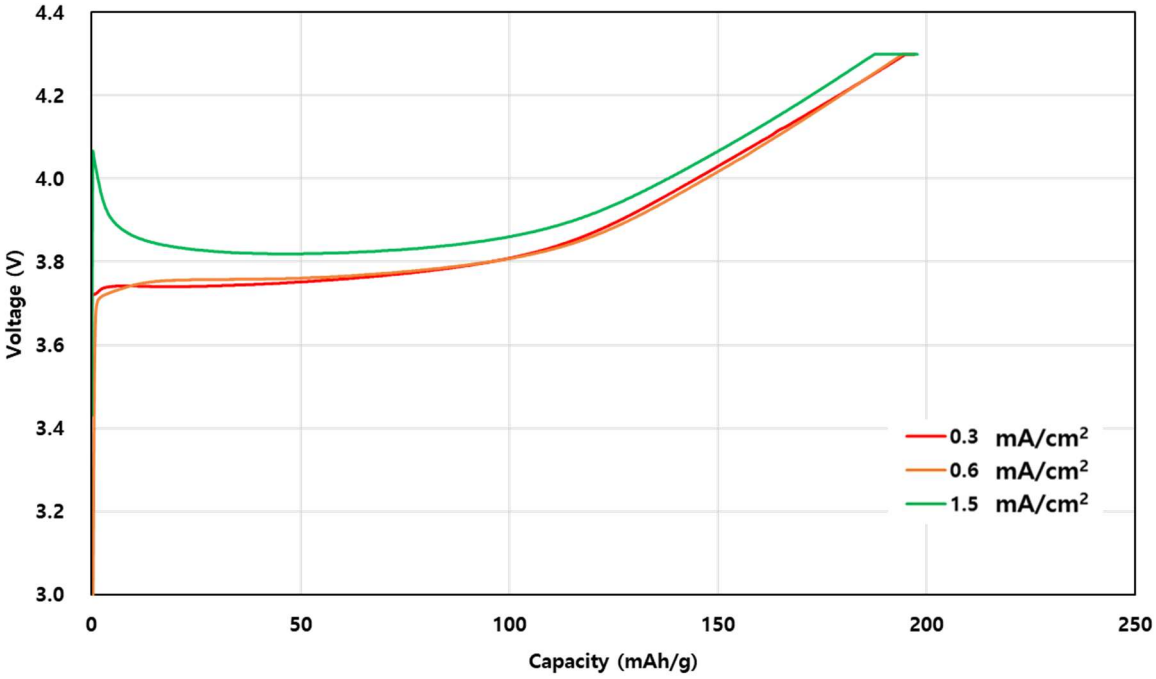

Figure 23 Voltage profile of NCM622 cathode material as current density.

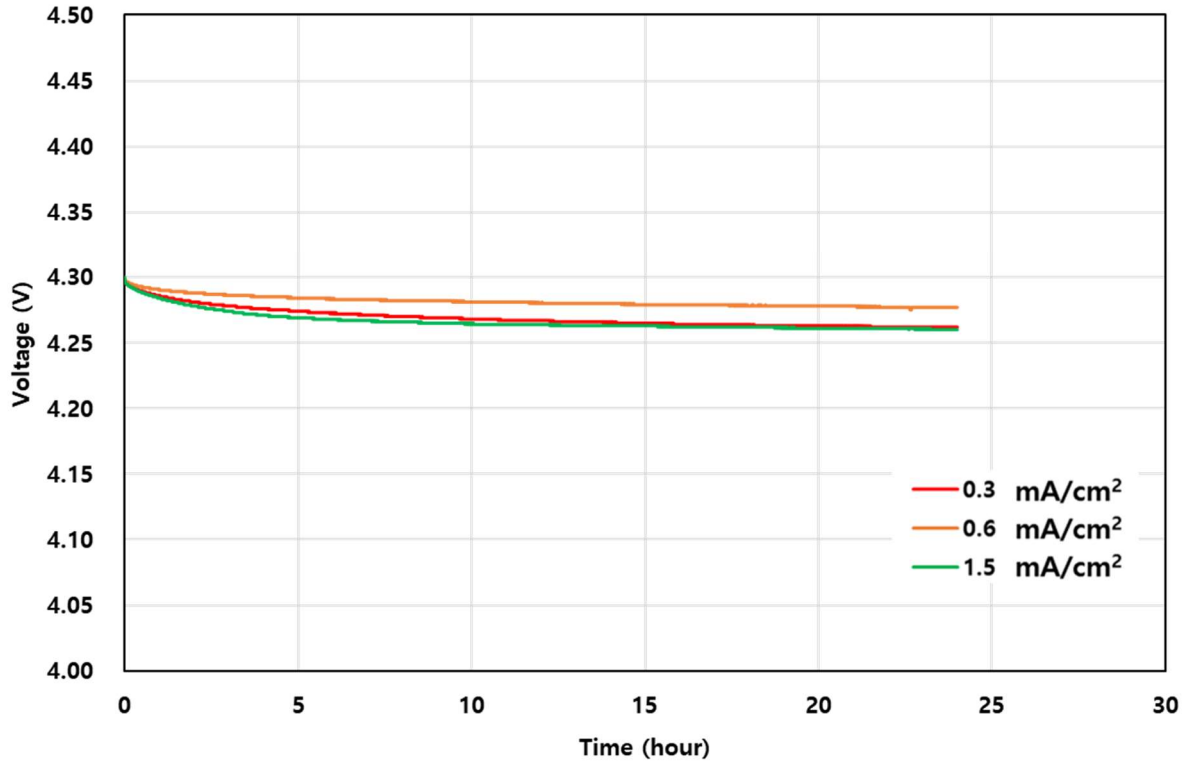

Figure 24 Voltage drop during rest after 4.3 V charging as current density.

3.2.2. Voltage drop by the internal short from Cu contamination after charging

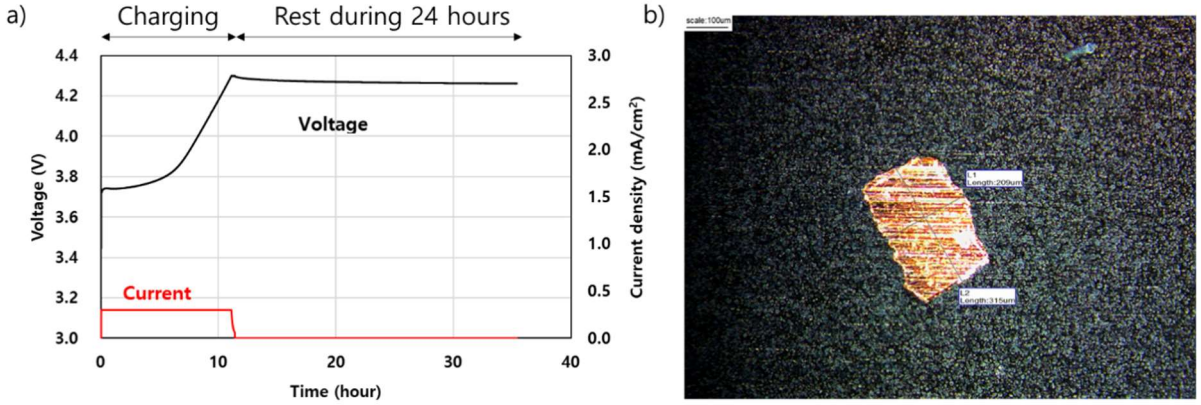

Figure 25 Experimental process for confirmation of voltage drop problem a), surface image of Cu-implanted cathode b).

To confirm the voltage drop caused by the internal short after charging, the experiment was performed as shown in figure 25 a). NCM622 half-cell was charged to 4.3 V and left to stand for 24 hours to confirm the voltage drop. Positive electrode with a Cu sheet on the surface was used to confirm the influence of Cu contamination as figure 25 b). The electrical quantity for dissolving of Cu sheets is few effects of capacity of NCM622 half-cell because electrical quantity for dissolving like several hundreds of micro-level Cu sheets was small about only 0.02 mAh in comparison with over 5 mAh capacity of bara NCM622 half-cell. Figure 26 shows difference of voltage profile in the presence or absence of Cu contamination on positive electrode. The initial potential of cathode at constant current charging is over 3.7 V. At 3.7 V, oxidation rate of Cu is about 1 mA/cm^2. That means, for dissolving all Cu contamination, 20 hours was needed. However, as potential of cathode increases, oxidation rate of Cu increases exponentially. After 3.9 V, only 2 minutes is required for dissolving all Cu contamination. The difference in capacity during constant current charging process is due to the occurrence of the internal short, not the electrical quantity for dissolving Cu because Cu contamination is all dissolved before 3.9 V of cathode potential. After charge state of 100 mAh/g, effect of the internal short increases, then difference of state of charge state has grown as there is Cu contamination or not. As cell was charged by externally applied current and the internal short by Cu contamination caused self-discharge of the cell continuously. After 4.3 V charging, the internal short by Cu led the voltage drop in the rest region. Figure 27 shows voltage drop phenomenon by the internal short of Cu. For 24 hours rest, voltage of half-cell without Cu contamination dropped to only 4.26 V after 4.3 V charging, potential of cathode with Cu contamination dropped to 3.81 V.

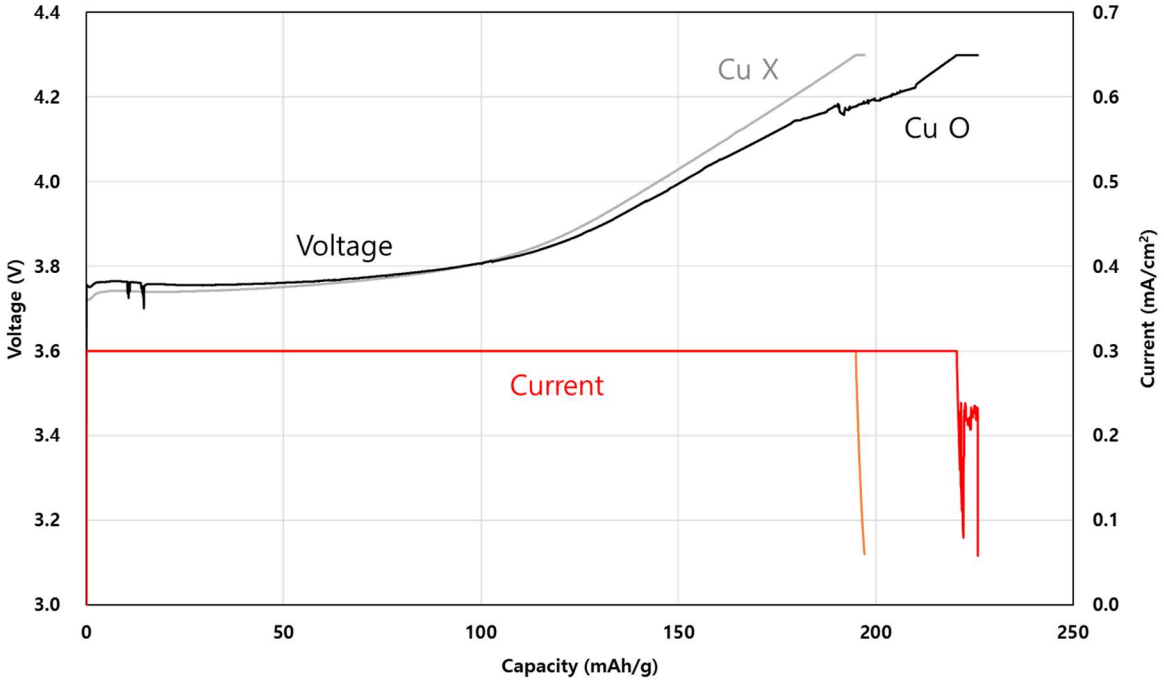

Figure 26 Voltage profile of NCM622 cathode during 0.3 mA/cm^2 current density charging as whether Cu contamination is present or not.

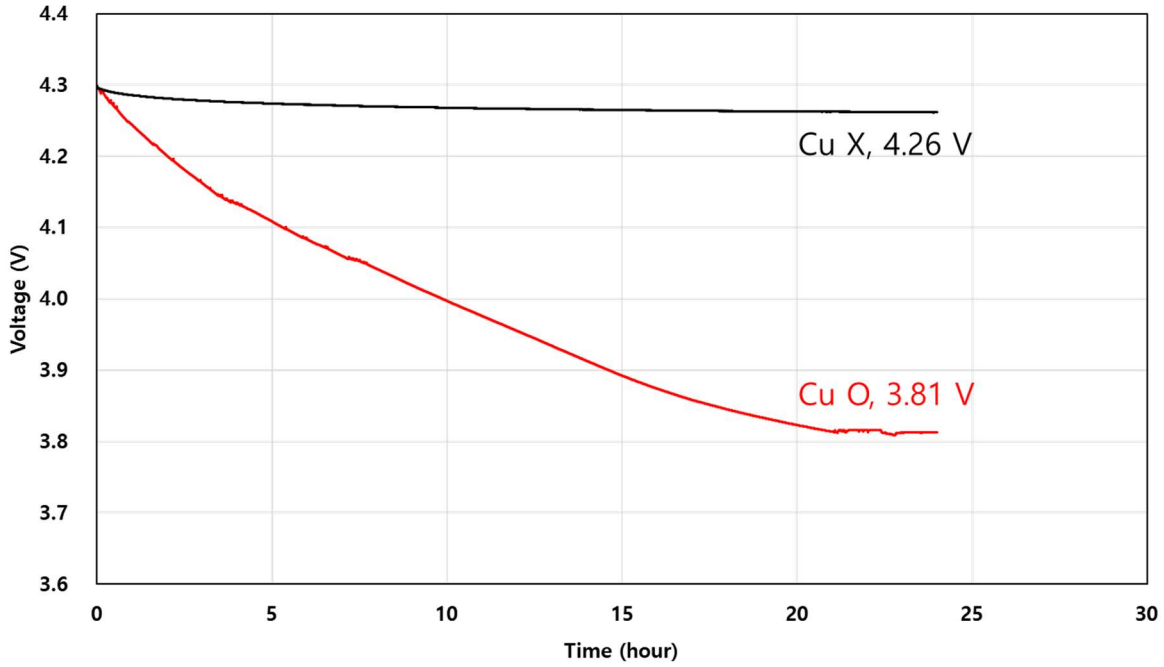

Figure 27 Voltage profile of NCM622 cathode during 24-hour rest after 0.3 mA/cm^2 current density charging as whether Cu contamination is present or not.

3.2.3. Difference of voltage drop as current density

Potential of cathode during charging was enough high for dissolving Cu contamination because potential of cathode material is over 3.5 V after starting charging at any current density. Any current density for charging of NCM622 half-cell, holding time over 3.9 V is higher than a few minutes, all Cu contamination will be dissolved. Figure 28, 29 shows difference of effects by the internal short of Cu contamination as current density. At low current density, effect of the internal short by Cu contamination was indicated at constant current charging. At 0.3 mA/cm^2 and 0.6 mA/cm^2, fluctuation of potential is confirmed at constant current charging. However, at 1.5 mA/cm^2, effect of the internal short during constant current was minimal. This phenomenon was occurred by difference between charge rate and leakage current. At low current density, leakage current by the internal short of Cu contamination influenced much more constant current charging process comparing with high rate current density.

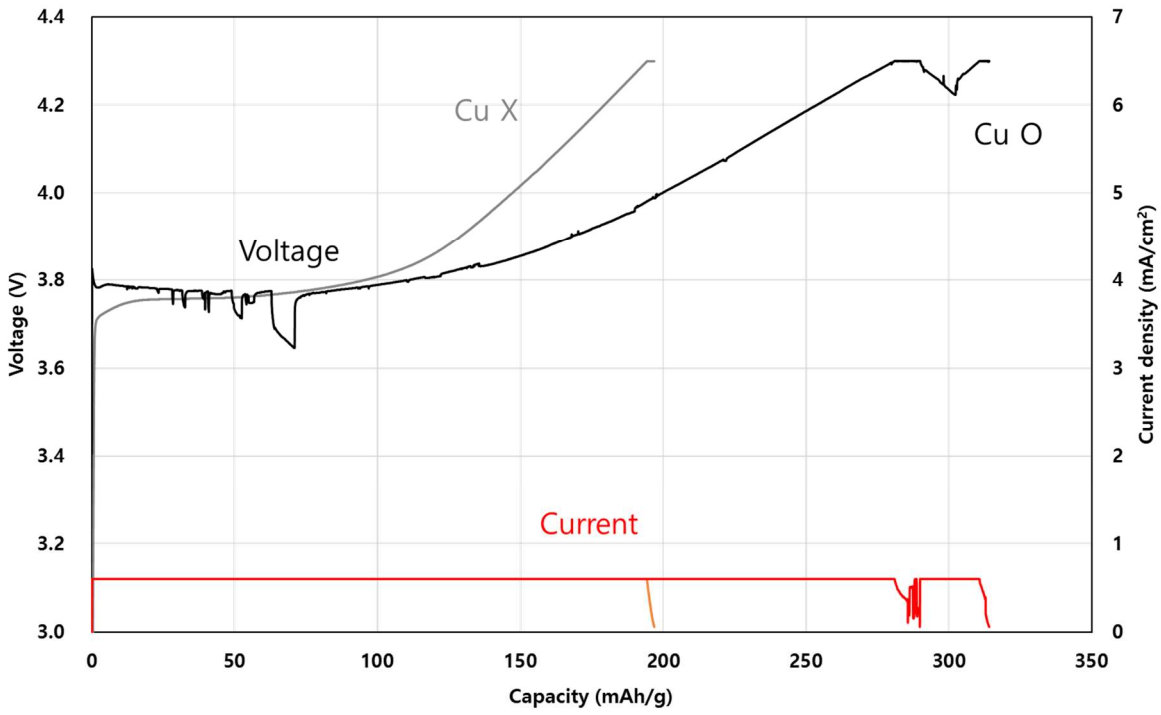

Figure 28 Voltage profile of NCM622 cathode during 0.6 mA/cm^2 current density charging as whether Cu contamination is present or not.

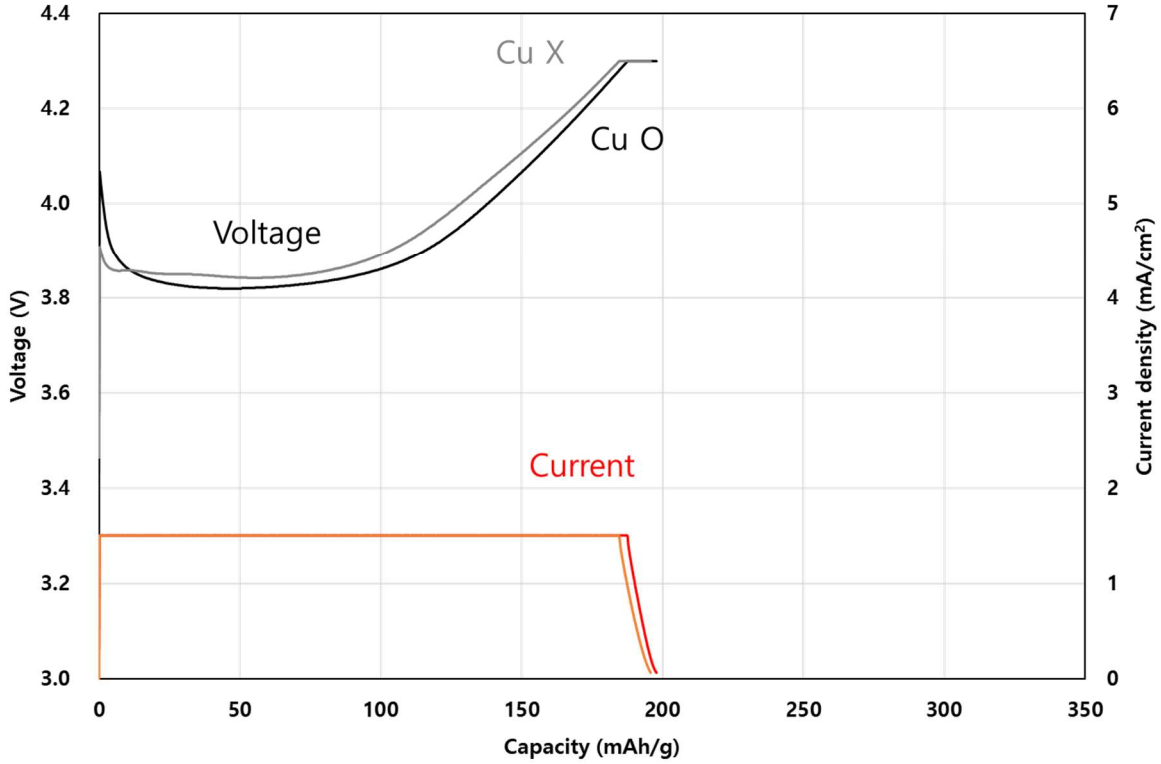

Figure 29 Voltage profile of NCM622 cathode during 1.5 mA/cm^2 current density charging as whether Cu contamination is present or not.

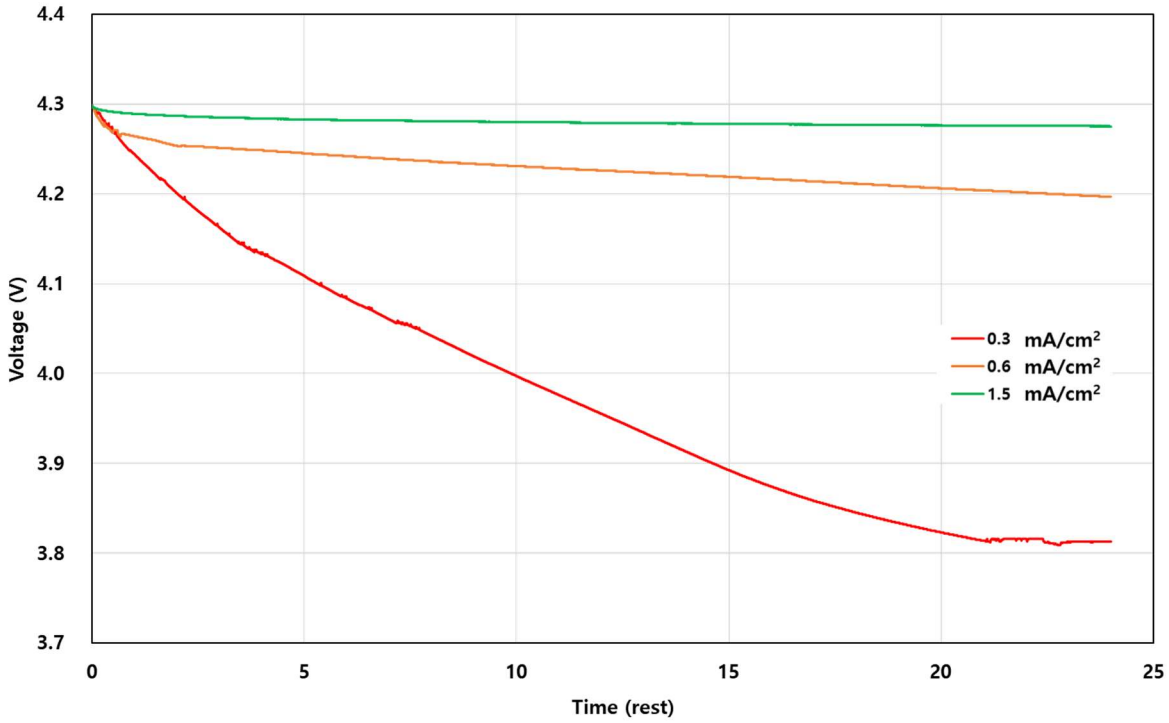

Figure 30 Voltage drop of NCM622 cathode as charging current density during 24-hour rest after 4.3 V charging when Cu contamination is present.

After charging, difference of potential drop rate was checked for 24 hours. Figure 30 shows difference of amount of potential drop according to current density at charging. As lower current density is applied, as bigger potential drop problems happened. To confirm state of charge as rest-time, Equilibrium potential of NCM622 cathode material at several states of charge was measured by GITT. Figure 31 shows equilibrium potential at region of state of charge from 4.3 to 3.6 V, under 3.6 V was not measured because of overpotential of half-cell. By using GITT data, variation of state of charge for 24 hours rest was observed. At 0.3 mA/cm^2, capacity loss was the highest, state of charge decreased to 57%, however, at 1.5 mA/cm^2, leakage current did not flow. Leakage current at any case of current density during constant current charging is under 1.5 mA/cm^2. The current density of 0.3 and 0.6 mA/cm^2 in the constant current charging was not large compared to leakage current, they are affected by the internal short. But at 1.5 mA/cm^2, leakage current is relatively small compared to charging current, effect of Cu contamination was smaller than effect at low current density. Figure 35 shows post-modern image of separator after 24-hour rest that indicates how much Cu was deposited on anode electrode and grown. Image of separator faced anode shows Cu contamination on cathode was dissolved enough and deposited on anode regardless of current density. However, degree of the internal short was difference as current density. As higher current density was applied, as lower degree of the internal short by Cu like image of separator faced cathode.

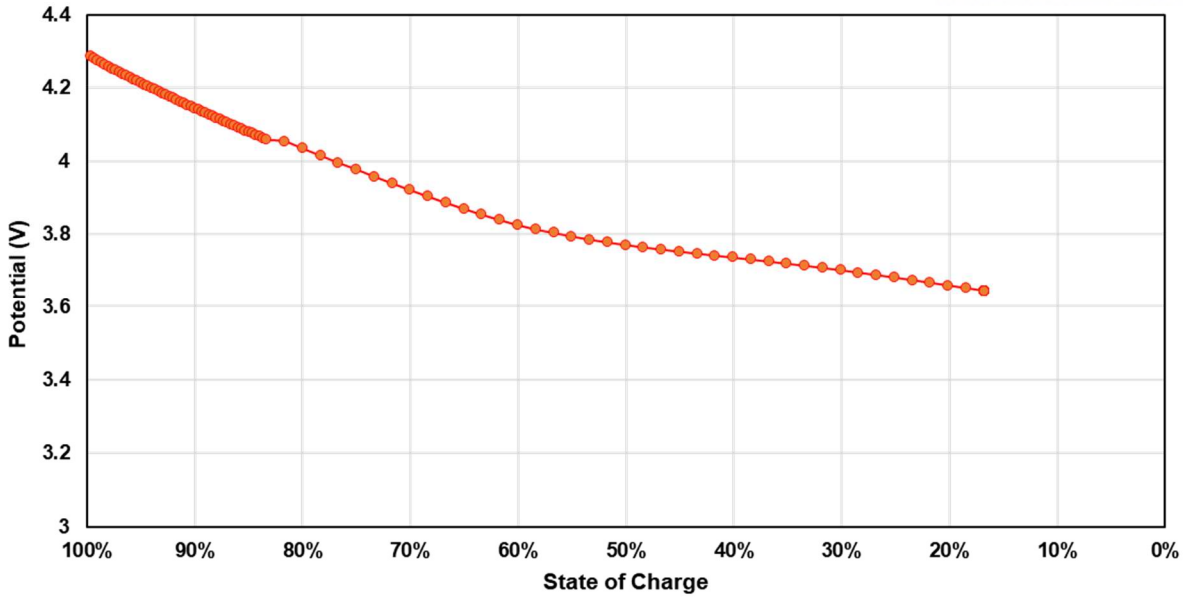

Figure 31 Open-circuit voltage of NCM622 cathode according to state of charge.

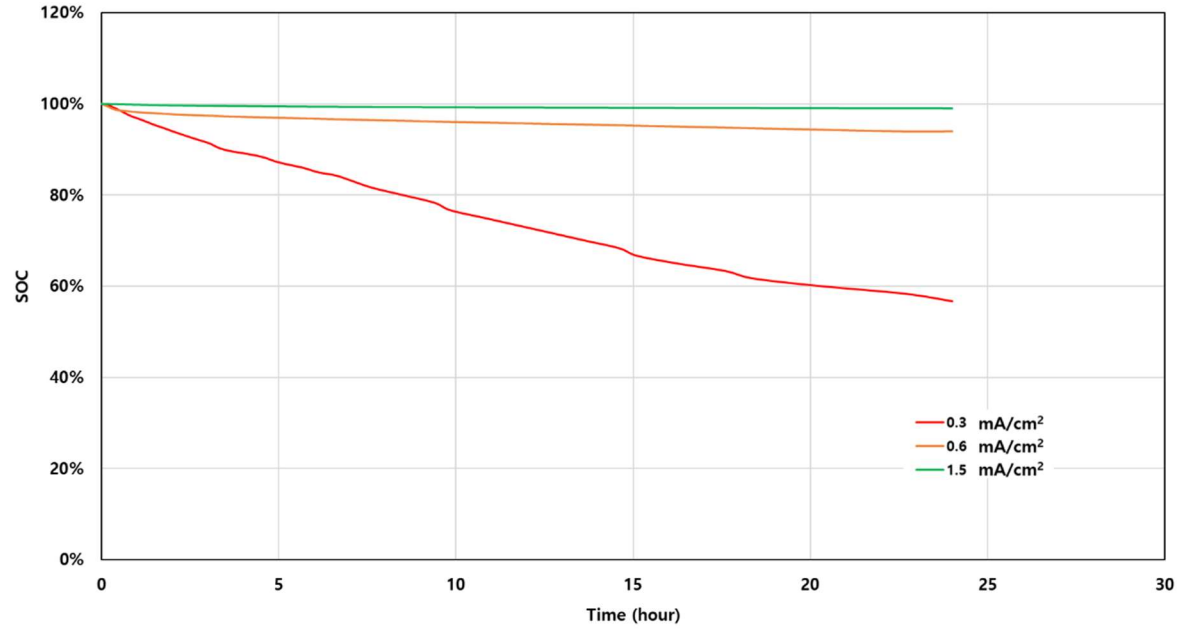

Figure 32 Degree of SOC change as charging current density during 24-hours rest after 4.2 V charging.

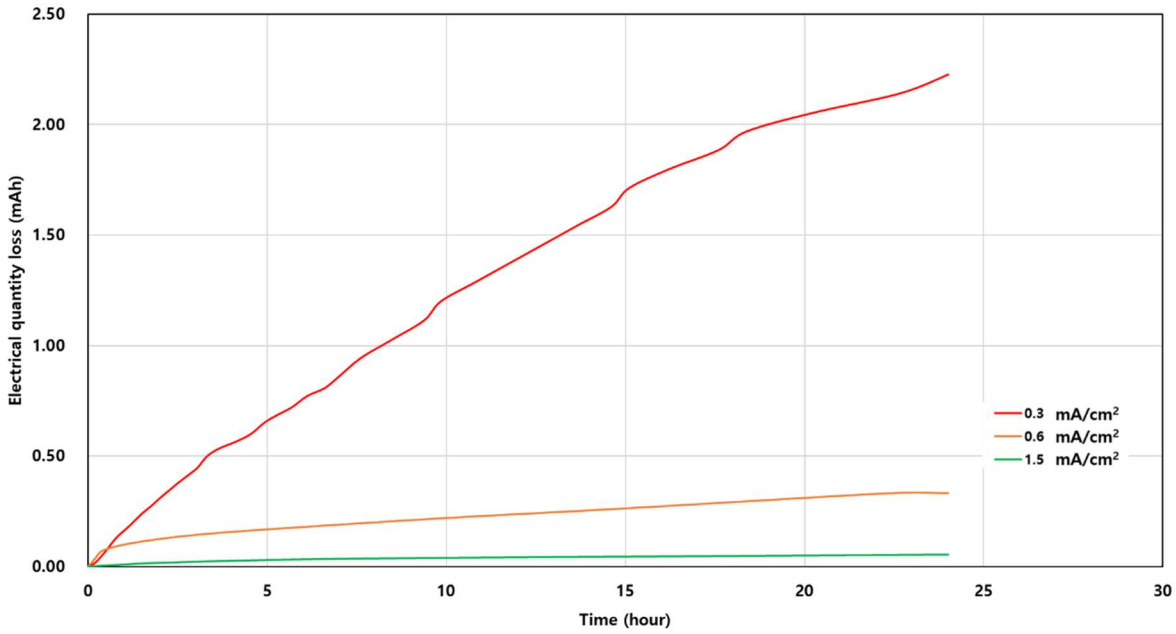

Figure 33 Electrical quantity loss as charging current density during 24-hours rest after 4.2 V charging

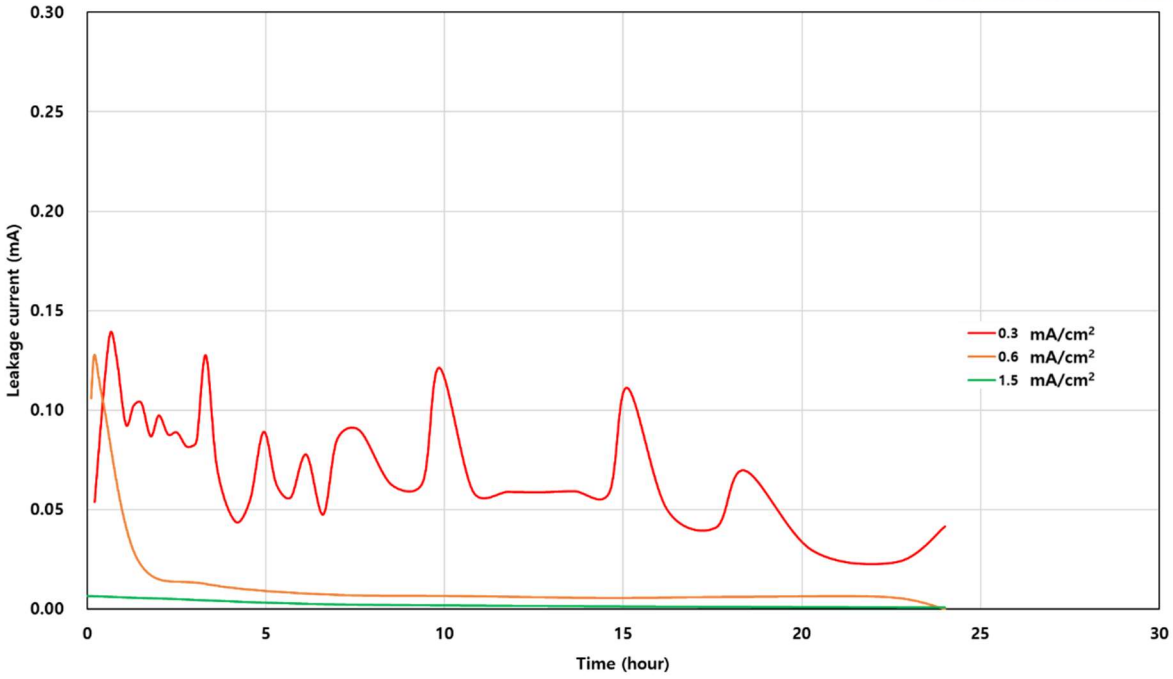

Figure 34 Leakage current as charging current density during 24-hours rest after 4.2 V charging

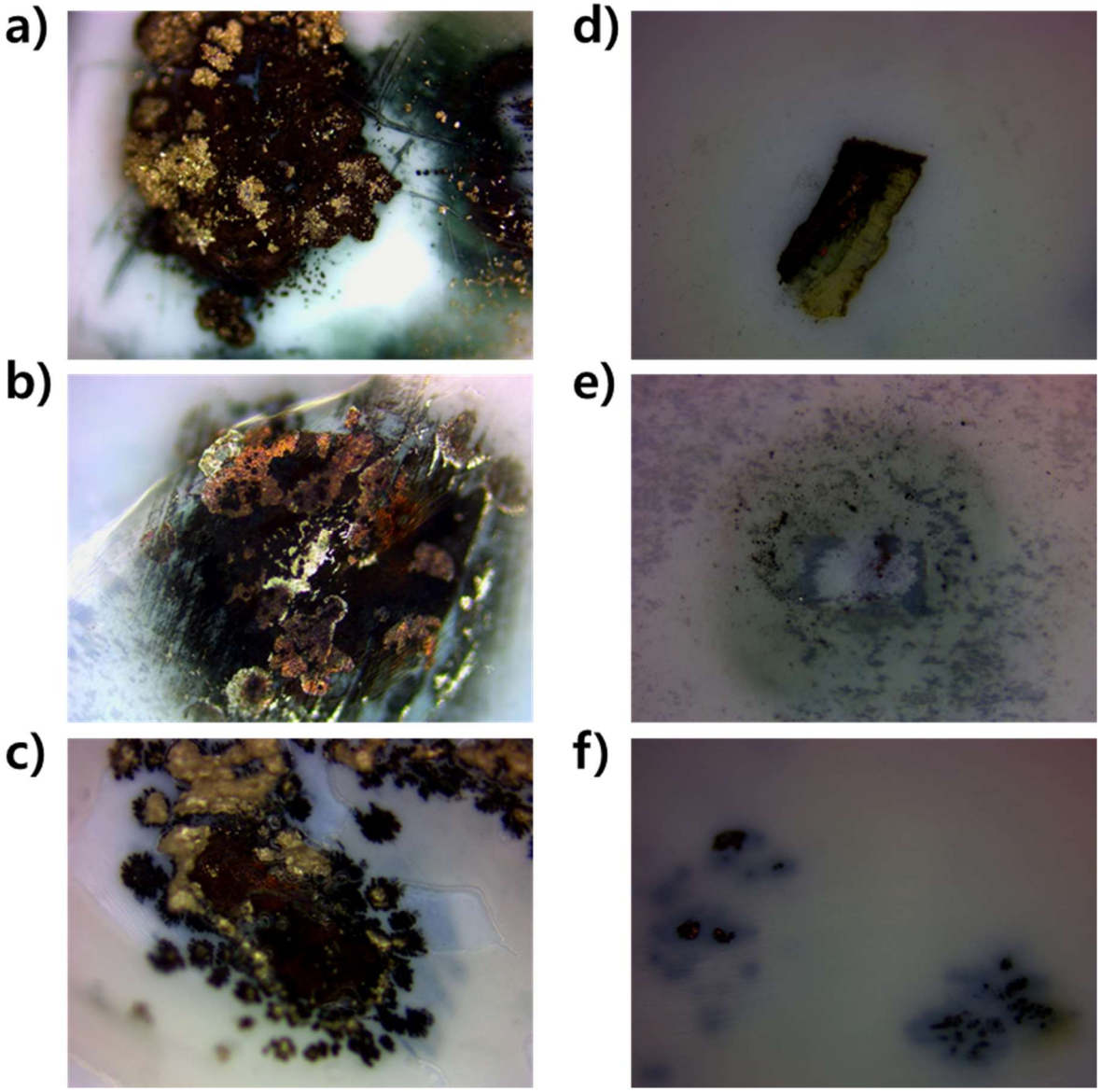

Figure 35 post-mortem photo of separator as different current after 4.3 V charging and 24-hour rest. Anode faced separator of NCM622 half-cell applied a) 0.3 mA/cm^2, b) 0.6mA/cm^2 and c) 1.5mA/cm^2, cathode faced separator of NCM622 half-cell applied d) 0.3 mA/cm^2, b) 0.6mA/cm^2 and c) 1.5mA/cm^2 during constant current.

IV. Conclusion

In this work, the effect of the current density on potential drop problems by Cu contamination was observed. Cu contamination on surface of cathode was dissolved during charging process and deposited on surface of anode. This Cu deposition makes the internal short in cell, leads self-discharging. As current density increases, effect of Cu contamination decreases. Leakage current influences constant current charging process at low current rate charging because difference between leakage current and charging current is small. But high current rate charging, effect of the internal short is minimal. Low potential area by the internal short is small at high current rate because the time of spent current by the internal short is short. Low potential area was charged during constant voltage charging, contacted Cu at cathode surface will be dissolved again, the internal short will be decreased. High rate charging is more effective than low rate charging for reducing of internal short induced Cu contaminations' dissolution and deposition.

V. Reference

1. Dunn, B.; Kamath, H.; Tarascon, J.-M., Electrical Energy Storage for the Grid: A Battery of Choices. **2011,** *334* (6058), 928-935.
2. Kuwabara, J.; Sato, K., In situ Observation of the Electrochemical Dissolution and Deposition of Copper Contaminations in Li-Ion Batteries. **2017,** *75* (20), 47-59.
3. Fear, C.; Juarez-Robles, D.; Jeevarajan, J. A.; Mukherjee, P. P., Elucidating Copper Dissolution Phenomenon in Li-Ion Cells under Overdischarge Extremes. **2018,** *165* (9), A1639-A1647.
4. Guo, R.; Lu, L.; Ouyang, M.; Feng, X., Mechanism of the entire overdischarge process and overdischarge-induced internal short circuit in lithium-ion batteries. *Scientific Reports* **2016,** *6*, 30248.
5. Lai, X.; Zheng, Y.; Zhou, L.; Gao, W., Electrical behavior of overdischarge-induced internal short circuit in lithium-ion cells. *Electrochimica Acta* **2018,** *278*, 245-254.
6. Seo, M.; Goh, T.; Park, M.; Kim, S., Detection Method for Soft Internal Short Circuit in Lithium-Ion Battery Pack by Extracting Open Circuit Voltage of Faulted Cell. **2018,** *11* (7), 1669.
7. Orendorff, C. J.; Roth, E. P.; Nagasubramanian, G., Experimental triggers for internal short circuits in lithium-ion cells. *Journal of Power Sources* **2011,** *196* (15), 6554-6558.
8. Zhang, M.; Du, J.; Liu, L.; Stefanopoulou, A.; Siegel, J.; Lu, L.; He, X.; Xie, X.; Ouyang, M., Internal Short Circuit Trigger Method for Lithium-Ion Battery Based on Shape Memory Alloy. **2017,** *164* (13), A3038-A3044.
9. Xu, J.; Wu, Y.; Yin, S., Investigation of effects of design parameters on the internal short-circuit in cylindrical lithium-ion batteries. *RSC Advances* **2017,** *7* (24), 14360-14371.
10. Kim, Y.-S.; Lee, S.-H.; Son, M.-Y.; Jung, Y. M.; Song, H.-K.; Lee, H., Succinonitrile as a Corrosion Inhibitor of Copper Current Collectors for Overdischarge Protection of Lithium Ion Batteries. *ACS Applied Materials & Interfaces* **2014,** *6* (3), 2039-2043.
11. Maleki, H.; Howard, J. N., Effects of overdischarge on performance and thermal stability of a Li-ion cell. *Journal of Power Sources* **2006,** *160* (2), 1395-1402.
12. Wu, C.; Sun, J.; Zhu, C.; Ge, Y.; Zhao, Y. In *Research on Overcharge and Overdischarge Effect on Lithium-Ion Batteries*, 2015 IEEE Vehicle Power and Propulsion Conference (VPPC), 19-22 Oct. 2015; 2015; pp 1-6.
13. Fuentevilla, D.; Hendricks, C.; Mansour, A., Quantifying the Impact of Overdischarge on Large Format Lithium-Ion Cells. **2015,** *69* (20), 1-4.

VI. Acknowledgement

This work was supported by Samsung SDI Co., Ltd., under SDI-UNIST Strategic Joint Research Programs.

Special thanks to dissertation committee assistant referees, Prof. Hyun-Kon Song and Prof. Hyun-Wook Lee.

Lastly, I would like to express my sincere appreciation to Prof. Kyeong-Min Jeong.